Quaternary International 713 (2024) 109573

Contents lists available at ScienceDirect

Quaternary International

journal homepage: www.elsevier.com/locate/quaint

Paleobiology and paleoecology of the woolly rhinoceros (*Coelodonta antiquitatis*) in Northern and Central Europe: New insights from multi-proxy data

Manon Hullot [a,b,*], Céline Martin [c], Cécile Blondel [d], Damien Becker [e,f], Gertrud E. Rössner [b,g]

[a] *Centre de recherche en paléontologie Paris (CNRS, MNHN, Sorbonne Université), Département Origines et Évolution, Muséum national d'Histoire naturelle, case postale 38, 57 rue Cuvier, F-75231, Paris, cedex 05, France*
[b] *Staatliche Naturwissenschaftliche Sammlungen Bayerns – Bayerische Staatssammlung für Paläontologie und Geologie, Richard-Wagner-Straße 10, 80333, Munich, Germany*
[c] *Géosciences Montpellier, Université de Montpellier Bât 22 – Place Eugène Bataillon, 34090, Montpellier, France*
[d] *PALEVOPRIM Poitiers, Université de Poitiers Bât B35 – TSA 51106, 6 rue Michel Brunet, 86073, Poitiers, France*
[e] *JURASSICA Museum, Route de Fontenais 21, 2900, Porrentruy, Switzerland*
[f] *Department of Geosciences, University of Fribourg, Chemin du Musée 6, 1700, Fribourg, Switzerland*
[g] *Department für Geo- und Umweltwissenschaften, Paläontologie & Geobiologie, Ludwig-Maximilians-Universität München, Richard-Wagner-Straße 10, 80333, Munich, Germany*

ARTICLE INFO

Keywords:
Würm-Weichselian glaciation
Pleistocene
Dental wear
Stable isotopy
Hypoplasia
Body mass

ABSTRACT

The woolly rhinoceros, *Coelodonta antiquitatis*, was an emblematic component of Pleistocene faunas in Eurasia, which went extinct around ca. 12.5 ky BP. The loss of its tundra-steppe habitat due to climatic changes is considered the main cause for its extinction, whereas human impact was limited. In this study, we investigated the paleobiology and paleoecology of *C. antiquitatis* during the last glacial interval (Würm/Weichselian; 130 to 11.7 kya). We explored evolutionary trends for diet, physiology, and habitat via dental wear, enamel hypoplasia, body mass, age structure, mortality curves and stable isotopes (carbon and oxygen). Our results confirmed that *C. antiquitatis* was a large-sized species, with body mass around 2000–2500 kg, and with C_3 grazing or mixed-feeding habits. Age structure and mortality curves revealed potential sampling and/or taphonomical biases at a few localities (e.g., Brixham cave, Ofnethöhle, North Sea), and indicated several vulnerability periods (birth, weaning, cow-calf separation/maturity) also retrieved by hypoplasia analyses. We observed some spatio-temporal fluctuations of body mass (1850–2955 kg), dietary preferences (strict to variable grazing) and hypoplasia prevalence (7.41–47.06 %) of *C. antiquitatis* depending on the locality, but correlation to specific climatic events (stadials-interstadials) is difficult without exact datation. These variations were however limited, highlighting a rather strict climatic niche and suggesting a high vulnerability to climatic and vegetation changes.

1. Introduction

The Quaternary is marked by glacial-interglacial cycles and is a crucial period in human evolution, as the first hominins arrived in Eurasia during the Early Pleistocene (Ferring et al., 2011). The most recent of these cycles (Riss-Würm interglacial and Würm glaciation in Alpine domain, Eemian interglacial and Weichselian glaciation in Northern Europe) spanned over approximately 120 ky (from 130 to 11.7 kya; Gibbard and Head, 2020). The last glacial interval (Würmian/-Weichselian) witnessed the Late Quaternary Extinctions (LQE; ~50-4 kya), a global extinction event of the Pleistocene mammalian megafauna (>44 kg; Stuart and Lister, 2007). The LQE have been much studied in the last decades and a great effort for dating localities in Europe provides a well-calibrated time scale of extinction for the concerned species (Stuart and Lister, 2012; Turvey et al., 2021). However, the drivers of the LQE are still hotly debated and especially the relative role of humans and of climate changes (Barnosky et al., 2004; Koch and Barnosky, 2006).

Concerning Rhinocerotidae, the LQE corresponded to the disappearance of the last representatives of the family in Northern Eurasia:

* Corresponding author. Centre de recherche en paléontologie Paris (CNRS, MNHN, Sorbonne Université), Département Origines et Évolution, Muséum national d'Histoire naturelle, case postale 38, 57 rue Cuvier, F-75231, Paris, cedex 05, France.
E-mail address: manon.hullot@gmail.com (M. Hullot).

https://doi.org/10.1016/j.quaint.2024.10.005
Received 17 July 2024; Received in revised form 30 September 2024; Accepted 6 October 2024
Available online 24 October 2024

Stephanorhinus hemitoechus (narrow-nosed rhinoceros) and *Elasmotherium sibiricum* (Siberian unicorn) extirpated around 40 ky BP (calibrated before present; Stuart and Lister, 2012; Pandolfi et al., 2017; Kosintsev et al., 2019), whereas the emblematic woolly rhinoceros *Coelodonta antiquitatis* went extinct around 14–12.5 ky BP (Stuart and Lister, 2012; Lord et al., 2020). The latter event is better studied than the former two, although less studied than the extinction of the frequently associated woolly mammoth (*Mammuthus primigenius*; Kuzmin, 2010). Climate has often been proposed as the main driver of the extinction of the woolly rhinoceros (Kuzmin, 2010; Stuart and Lister, 2012), however *C. antiquitatis* is considered to have declined well before its extinction, due to the progressive reduction of its habitat (tundra-steppe; Stuart and Lister, 2012). The species was still present in large parts of Eurasia until ~16 ky BP, but the fossil record attests of successive fragmentation and isolation of the populations, which suggests a coeval or fast extinction across the whole area (Lorenzen et al., 2011). Recently, this progressive decline has been reconsidered, as new genetic approaches (mitochondrial DNA) showed a population increase ~30 ky BP and demographic stability until close to the extinction of *C. antiquitatis* (Lord et al., 2020).

In order to understand the impact of climatic changes on *Coelodonta antiquitatis*, we explored the evolution of its paleobiology and paleoecology across Northern (United Kingdom, Belgium, Netherlands, Northern Germany) and Western (France, Southern Germany) Europe during the last glaciation event (Würm-Weichselian). We notably targeted localities close to the regional extinction of the species and tracked the spatio-temporal variations of the niche to estimate the flexibility and vulnerability of *C. antiquitatis*. To do so, we studied body mass (molar measurements), age structure and mortality curves (teeth wear stages), dietary preferences (dental wear and carbon isotopes), habitat (carbon and oxygen isotopes), and stress susceptibility (enamel hypoplasia).

2. Materials and methods

We studied dental material attributed to *C. antiquitatis* from 15 sites in Europe dating from the last glacial interval (Würm-Weichselian; Fig. 1, Supplementary A). Details on each locality can be found in Supplementary B. The material is curated at the following institutions: Archäologisches Forschungszentrum und Museum für menschliche Verhaltensevolution Monrepos, Germany (Gönnersdorf); Staatliche Naturwissenschaftliche Sammlungen Bayerns – Bayerische Staatssammlung für Paläontologie und Geologie Munich, Germany (Bruine Bank, Ofnethöhlen, Vogelherdhöhle, Weinberghöhlen bei Mauern); Institute of Natural Sciences Brussels, Belgium (Goyet's Third cave, Hofstade, Caverne de Marie-Jeanne); Museum für Ur-und Ortsgeschichte Bottrop, Germany (Knochenkies Bottrop); Museum d'Histoire Naturelle de Paris, France (Kent's cavern); Naturalis Leiden, Netherlands (Bruine Bank and various from North Sea); Natural History Museum of London, United Kingdom (Kent's cavern, Brixham cave); Staatlisches Museum für Naturkunde Stuttgart, Germany (Bocksteinhöhle, Göpfelsteinhöhle, Irpfelhöhle, Ofnethöhlen, Vogelherdhöhle); Université Lyon 1 Claude Bernard, France (Jaurens Nespouls). Although the material from most localities was curated at only one institution, some localities were scattered between multiple collections. In the latter case, we tried to include the material from as many collections as possible to provide the most complete insight for each locality, but it is possible that we missed some.

We used a multi-proxy approach to investigate the paleobiology and paleoecology, combining mortality curves, body mass estimation, enamel hypoplasia, stable carbon and oxygen isotopes, dental mesowear and microwear. The number of teeth studied for each method is detailed in Table 1 by locality. Each method is described thereafter.

2.1. Minimum number of individuals

The minimum number of individuals (MNI) is the smallest number of individuals of the same species that can be identified from a fossil assemblage. It is determined by the number of the most abundant anatomical element from the same body side (e.g., right astragali, left P4s). Here, the MNI was estimated on the dental material only, as the scope of the study was limited to teeth.

2.2. Mortality curves and age structure

Mortality curves display the number of individuals from a sample across different age categories defined. They are used in archeology and paleontology to reconstruct the age structure of a sample (Fernandez and Legendre, 2003; Bacon et al., 2018). For this study, we used the protocol of Hullot and Antoine (2020) for rhinocerotids' teeth. Mortality curves are built by following the steps thereafter.

- estimation of the wear stage (1–10) defined by Hillman-Smith et al. (1986) in the extant *Ceratotherium simum* (white rhinoceros) for each tooth;
- correlation to one or several age classes (I-XVI) corresponding to the wear observed for the locus concerned;
- equal weight given to each age class (1 if one, ½ if two, and so on);
- if the tooth is associated to others, grouping of all teeth as a single individual and proposition of an age class or combination of weighted classes for the group;
- construction of mortality curves from the weighted classes.

Age classes were then converted into percentages of lifespan using the age borders defined in *C. simum* (Hillman-Smith et al., 1986; Hullot and Antoine, 2020).The distribution in age classes was corrected as a histogram by dividing the number of specimens per age classes by the duration of the age classes.

The distribution between the different age classes can also give access to the age structure between the different ontogenetic stages. The ontogenetic stages are defined as follows by Hullot and Antoine (2020).

- 'juveniles' group individuals from birth to weaning, corresponding to age classes from I to V (1.5 months–3 years old in the extant white rhinoceros). This stage ends with the eruption of the first permanent teeth (m1/M1);
- 'subadults' are individuals between weaning and sexual maturity, here corresponding to age classes VI to VIII (3–7 years) and ending with the eruption of the last permanent teeth (m3/M3);
- 'adults' consist of individuals which are sexually mature, which correlates with age classes IX to XVI (7–40 years). This stage starts after the eruption of the last permanent teeth (m3/M3).

The age structure of our samples was compared to that of recent rhinoceros populations obtained through direct observations. This includes populations of: *Ceratotherium simum* at Kyle National Park (Zimbabwe; Pienaar, 1994) and at Hluhluwe-Umfolozi Game Reserve (South Africa; Pienaar, 1994), *Rhinoceros unicornis* at Chitwan National Park (Nepal; Laurie et al., 1983), and *Diceros bicornis* at Hluhluwe-Umfolozi Game Reserve (Mundy, 1984), Tsavo National Park (Kenya; Goddard, 1970), and in Zululand reserves (South Africa: Hluhluwe-Umfolozi, Mkuze and Ndumu Game Reserves; Hitchins, 1978). The age structure of *C. antiquitatis* from Fouvent (Late Pleistocene; France) was also compared to our samples (Fourvel et al., 2015).

2.3. Body mass estimations

Body mass has consequences on many physiological and ecological parameters (e.g., diet, metabolism, heat evacuation; Peters, 1983; Owen-Smith, 1988; Clauss et al., 2003). Its estimation in fossil species is complex, as it relies on indirect proxies and actualism (calibration of the equation on extant species). Many equations are available in the literature based on various dental and limb bone proxies for different taxa (see the review of Hopkins, 2018). Here, we used molars as body mass

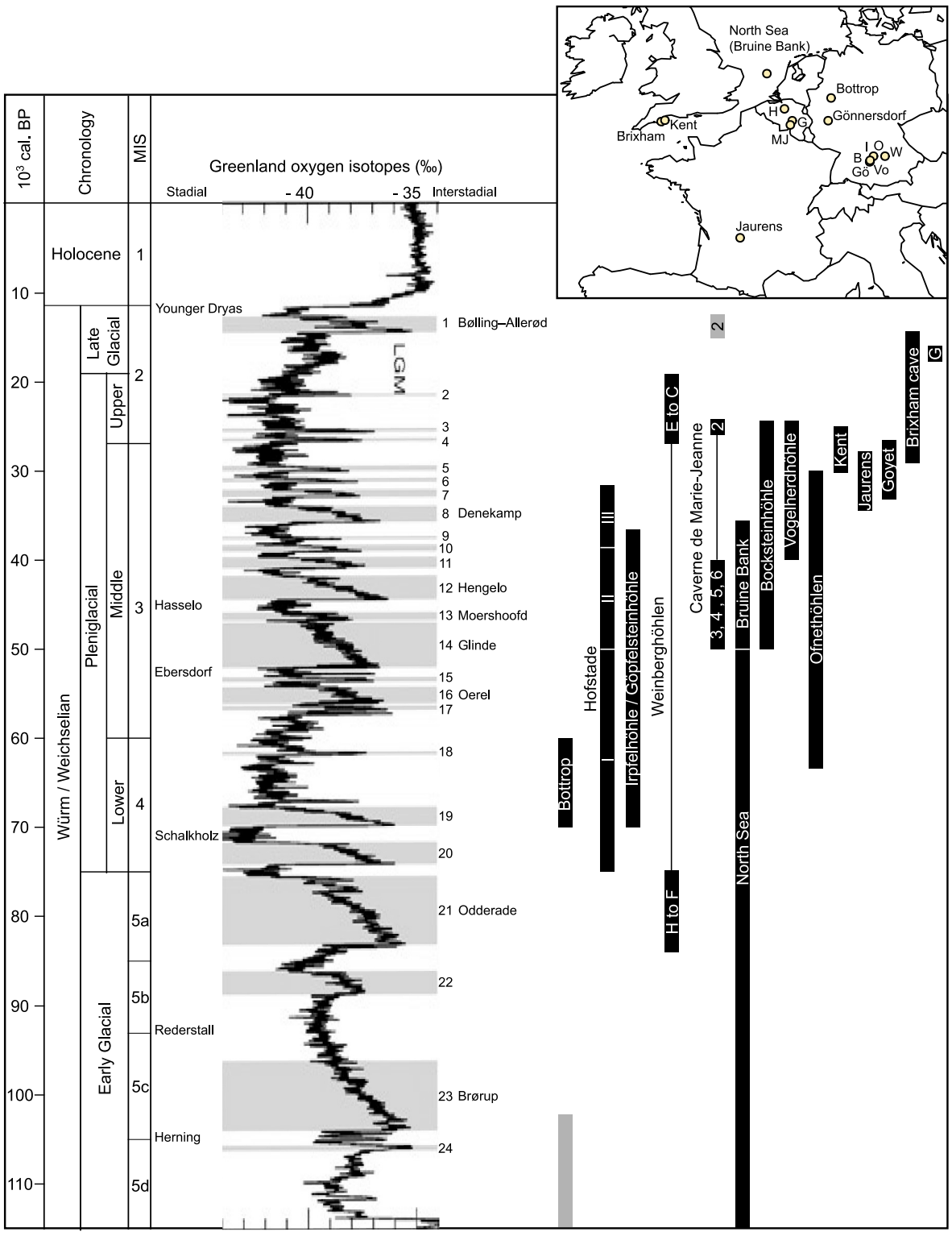

Fig. 1. Localization and chronology of the studied Late Pleistocene localities in Europe.
Abbreviations (map): B – Bocksteinhöhle, G – Goyet's third cave, Gö – Göpfelsteinhöhle, H – Hofstade, I – Irpfelhöhle, MJ – Caverne de Marie-Jeanne, O – Ofnethöhle, Vo – Vogelherdhöhle, W - Weinberghöhlen bei Mauern. Abbreviations (stratigraphical chart): G – Gönnersdorf, MIS – Marine Isotopes Stages. For localities: grey rectangles show alternative debated datings. Chronology according to the following references: von Koenigswald and Müller-Beck (1975); Guérin et al. (1979); Jansen and Drozdzewski (1986); Germonpré (1993); Hedges et al. (1996); Street and Terberger (2004); Mol et al. (2006); Boylan (2008); Conard and Bolus (2008); Stevens et al. (2009); Baales (2012); Brace et al. (2012); López-García et al. (2017); Çep et al. (2021). Greenland oxygen isotopes curve modified from Mogensen (2009).

Table 1
List of localities studied along with the number of teeth of *Coelodonta antiquitatis* included for each method.

	BM	Microwear		Mesowear	Hypoplasia	Isotopy
		Gr	Sh			
Gönnersdorf	–	–		–	–	2
Brixham cave	4	0	0	1	16	–
Jaurens	16	16	6	47	64	–
Goyet	73	9	5	12	337	15
Kent's cavern	55	4	1	53	258	–
Ofnethöhle	7	4	2	11	47	4
Vogelherdhöhle	–	2	2	2	15	2*
Bocksteinhöhle	3	3	1	4	17	3*
North Sea	80	6	5	45	262	–
Marie-Jeanne	27	9	2	27	188	–
Weinberghöhlen bei Mauern	5	2	0	3	33	–
Göpfelsteinhöhle	9	2	1	7	27	3
Irpfelhöhle	6	5	3	8	27	–
Hofstade	35	5	2	6	120	–
Knochenkies Bottrop	71	34	21	37	229	–

Abbreviations: BM for body mass in kg, Gr for grinding facet, Sh for shearing facet. The * indicates bulk isotopic data from the literature for Bocksteinhöhle and Vogelherdhöhle (Pushkina et al., 2014). Localities ordered chronologically (oldest to the bottom).

proxies, as we studied teeth for all other methods and as they are abundant and well preserved in the fossil record. The proxies and equations are detailed in Table 2 alongside with the corresponding references. For each equation, we obtained the mean body mass of *C. antiquitatis* at the locality (if several teeth were available for one individual, only one by locus was randomly selected for the mean calculation at the locality). We then used the median of the means of all proxies to report for each locality.

2.4. Enamel hypoplasia: stress proxy

Enamel hypoplasia is a very common developmental defect of the tooth crown. This kind of defect is permanent (as enamel is not remodeled during life), sensitive, but individual, and non-specific (Guatelli-Steinberg, 2001). Many factors have been proposed to cause hypoplasia including birth (Mead, 1999; Upex and Dobney, 2012), weaning (Goodman and Rose, 1991; Dobney and Ervynck, 2000), diseases (Niven et al., 2004), or nutritional stress (Goodman and Rose, 1991; Upex and Dobney, 2012). The study of these defects is mostly conducted with the naked eye, as it is faster, cheaper, and less prone to false positives than microscopy approaches (Hullot and Antoine, 2022). This approach starts with the macroscopical spotting and identification of the defects according to the *Fédération Dentaire Internationale* (pit, linear, or aplasia). Then several parameters are measured, including the distance of the defect to the root and the width of the defect (when possible), respectively linked to the timing of formation, and the duration and severity of the defect (Goodman and Rose, 1990; Ensor and Irish, 1995; Skinner and Skinner, 2017). Other information is recorded as well, such as the number of defects and their type, the localization on the tooth crown, or the degree of severity (see Fig. 1 in Supplementary B).

Table 2
List of the tooth loci and the associated equations with the respective dental proxy used to estimate body mass in this study.

Locus	Equation	Reference
m1		
	ln(m) = 1.5133* ln(m1 length* width) + 3.6515	Legendre (1989)
	log(m) = 3.26* log(m1 length/10) + 1.337	Janis (1990)
m2		
	log(m) = 3.2* log(m2 length/10) + 1.13	Janis (1990)
	log(m) = 3.07* log(m2 length) + 1.07	Damuth (1990)
M1		
	ln(m) = 3.19* ln(M1 length) + 2.1	Fortelius and Kappelman (1993)
M2		
	log(m) = 3.18* log(M2 length/10) + 1.091	Janis (1990)
	log(m) = 3.03* log(M2 length) + 1.06	Damuth (1990)
	ln(m) = 3.09* ln(M2 length) + 2.14	Fortelius and Kappelman (1993)

Measurements are in mm for all equations and give body mass in kg for Janis (1990) and in g otherwise. Upper case for upper teeth (M1/M2) and lowercase for lower ones (m1/m2).

2.5. Dental wear: mesowear and microwear

Dental meso- and microwear are often used in paleontology to infer dietary preferences at different time scales (e.g., Danowitz et al., 2016; Xafis et al., 2020; Kelly et al., 2021; Berlioz et al., 2022; Uzunidis and Rivals, 2023). Mesowear is the scoring of gross dental wear cumulative over an individual's life time (Fortelius and Solounias, 2000; Ackermans et al., 2020) on upper molars of large herbivores (cusp shape and occlusal relief: Fortelius and Solounias, 2000), used to infer dietary preferences. Here, we scored the paracone of *C. antiquitatis* molars using the mesowear ruler developed by Mihlbachler et al. (2011). This method was initially developed on equids, which are close relatives of rhinocerotids with similar lophodont molars and digestive tracts (Clauss et al., 2005; Taylor et al., 2013; Schultz et al., 2020), but is perfectly applicable to rhinoceroses (Mihlbachler et al., 2018; Hullot et al., 2021). The ruler ranges from 0 (high sharp) to 6 (low blunt; see Fig. 2 Supplementary B). With this approach, browsers have low scores (extant species between 0 and 2) and grazers high ones (2.09–5.47), while mixed-feeders have intermediate values (0.4–2.74; Mihlbachler et al., 2011). As mesowear is impacted both by age and hypsodonty (Fortelius and Solounias, 2000), we only scored upper molars with an average wear (wear stages from 4 to 7 defined by Hillman-Smith et al. (1986), and tracked the hypsodonty index (height of m3 divided by its width; Janis, 1988). The hypsodonty index (HI) differentiates brachydont (HI < 1.5), mesodont (HI > 1.5 and < 3.0), hypsodont (HI > 3.0 and < 4.5), and highly hypsodont (HI > 4.5) teeth (Janis, 1988).

Dental microwear is a short-term (days to weeks) proxy of the diet, that correlates wear patterns at the enamel surface with dietary categories (Gordon, 1982; Teaford and Walker, 1984; Teaford and Oyen, 1989). In this study, we followed a protocol adapted from Scott et al. (2005) and detailed thereafter. We studied well-preserved wear facets on the same enamel band near the protocone, protoconid or hypoconid of molars (see Fig. 3 Supplementary B), and documenting both phases of the mastication (grinding and shearing; Fortelius, 1982; Ballatore et al., 2017). The wear facets were cleaned twice using a cotton swab soaked in acetone to remove glue, dirt, and grit before silicon molding (Coltene Whaledent PRESIDENT The Original Regular Body, ref. 60019939). Then, the molded facet was cut out of the mold, put flat under a Leica Map DCM8 profilometer (TRIDENT, PALEVOPRIM Poitiers), and scanned using white light confocal technology with a 100 × objective (Leica Microsystems; Numerical aperture: 0.90; working distance: 0.9 mm). Specimens presenting taphonomical alterations were excluded from the analyses (see details on identification and some examples of excluded surfaces in Supplementary B). The scans obtained were then pre-treated under LeicaMap (v.8.2; Leica Microsystems). The pre-treatment included the inversion of the surface (as they come from negative replica), the replacement of the missing points (i.e, non-measured, less than 1%) by the mean of the neighboring points, the removal of aberrant peaks, the leveling of the surface, the removal of form (polynomial of

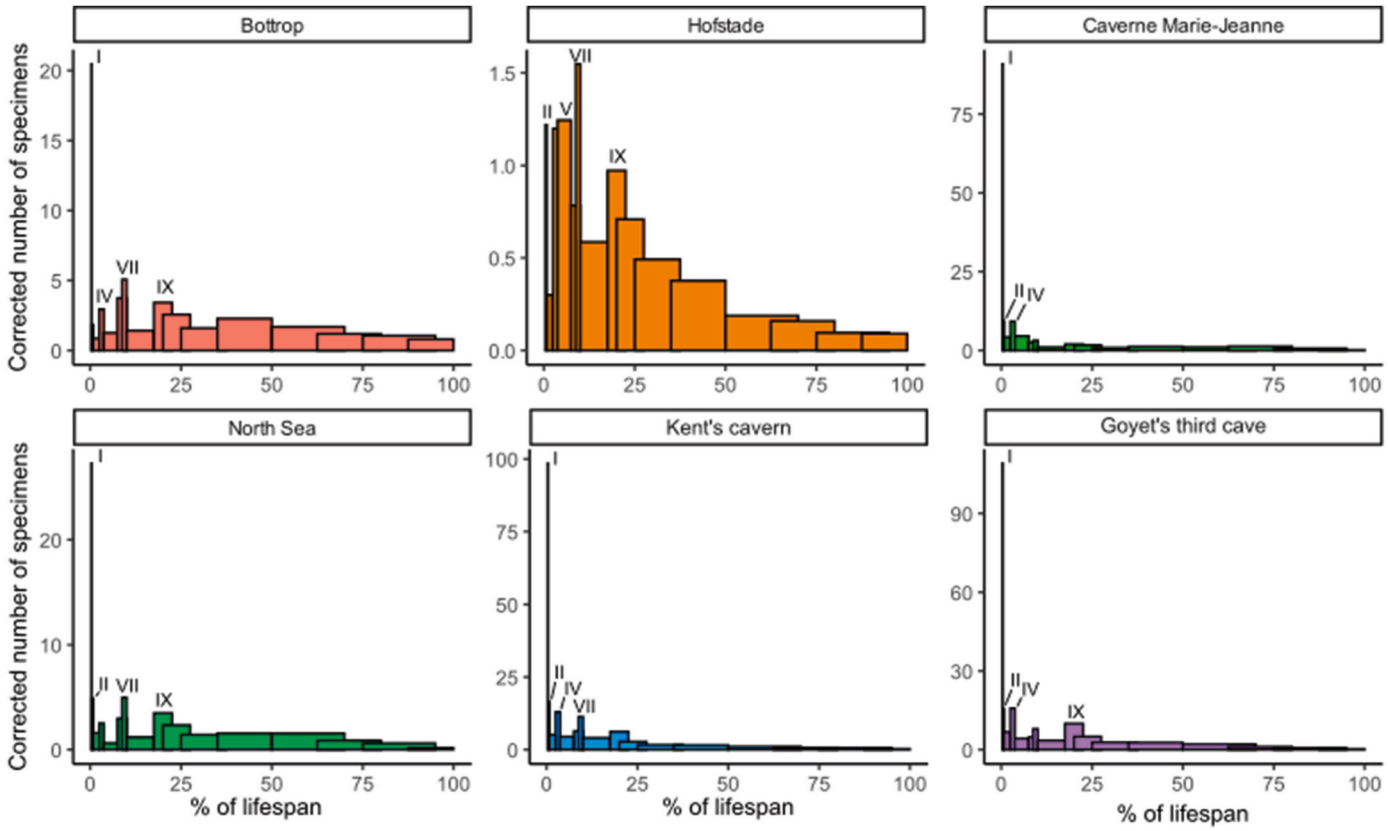

Fig. 2. Mortality profiles of *Coelodonta antiquitatis* samples at the different localities.
X-axis: age classes converted to percentage of lifespan, Y-axis: corrected number of individuals (observed number divided by duration of age class). Age classes peaking are indicated in each graph. Localities ordered chronologically from oldest (top left) to youngest (bottom right).

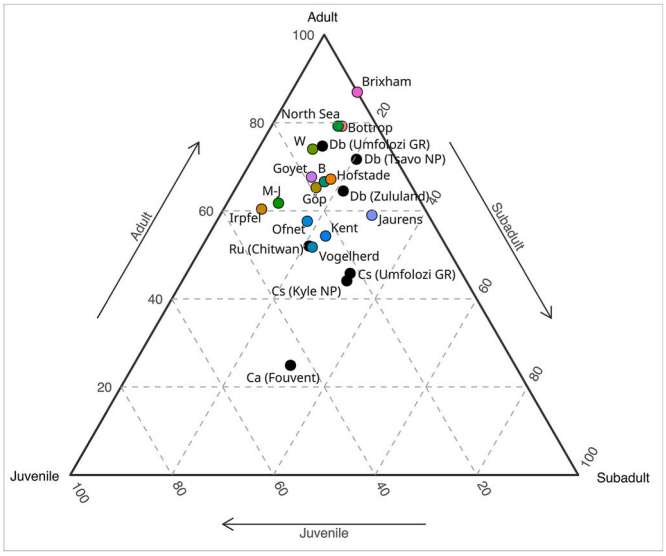

Fig. 3. Age structure of the *Coelodonta antiquitatis* sample at the localities studied compared to that at Fouvent and in extant rhinoceroses' populations.
In black: extant species' populations and Fouvent (MIS3, Pleistocene; France). References: Tsavo National Park (Kenya; Goddard, 1970), Zululand, Hluhluwe-Umfolozi Game Reserve (South Africa; Pienaar, 1994), Kyle National Park (Zimbabwe; Pienaar, 1994), Chitwan National Park (Nepal; Laurie et al., 1983), Fouvent (Late Pleistocene, France; Fourvel et al., 2015).
Abbreviations: B – Bocksteinhöhle, Ca – *Coelodonta antiquitatis*, Cs – *Ceratotherium simum*, Db – *Diceros bicornis*, Göp – Göpfelsteinhöhle, GR – Game Reserve, M-J – Caverne de Marie-Jeanne, NP – National Park, Ru – *Rhinoceros unicornis*, W – Weinberghöhlen. Color code by locality.

degree 8), and the selection of a 200 × 200 μm area (1551 × 1551 pixels) to be used for the analyses. Several ISO (Francisco et al., 2018) and scale-sensitive fractal analyses (Scott et al., 2006) parameters were extracted using MountainsMaps® (v.8.2). Our study will focus on the following.

- Str is a spatial parameter of the international standard ISO 25178 (specification and measurement of 3D surface textures) indicative of the surface anisotropy (i.e., orientation concentration of surface roughness). It is the ratio of Rmin/Rmax, where Rmin and Rmax are respectively the minor and major axes of the intersection ellipse between the plane z = s with the auto-correlation function f_{ACF}(tx, ty). Rmin is the auto-correlation length, i.e. the horizontal distance of the f_{ACF}(tx, ty) which decays fastest to a specified value s between 0 and 1. Here, we considered s = 0.5. Low values of Str indicate strong anisotropy;
- Asfc (area-scale fractal complexity) measures the complexity of the surface, which is the roughness at a given scale;
- heterogeneity of the complexity (HAsfc) gives information on the variation of complexity at a given scale (here 3 × 3 and 9 × 9) within the studied zone (200 × 200 μm).

2.6. Carbon and oxygen stable isotopes of the carbonates from rhinocerotids' enamel

Stable isotopes are very powerful tools frequently used in paleontology to infer dietary preferences (C_3-C_4 preferences) and habitat conditions (e.g., Bentaleb et al., 2006; Stefaniak et al., 2020; Zanazzi et al., 2022). Here, we have focused on the carbon and oxygen content from the carbonates of tooth enamel of *C. antiquitatis*, as both can be studied at the same time (faster and cheaper).

Due to sampling restrictions (lack of specimens, preservation, costs), only teeth from four localities were analyzed (Göpfelsteinhöhle, Gönnersdorf, Ofnethöhle, Goyet's third cave). Additionally, we included data from the literature (Pushkina et al., 2014) for two more (Bocksteinhöhle and Vogelherdhöle). Serial sampling was done along the crown of identified isolated teeth or fragments, preferably from third molars to avoid pre-weaning or weaning signal. Before the sampling, the zone was cleaned mechanically using a Dremmel© equipped with a diamond tip. With the same tool, we collected about 2 mg of enamel powder. For the analyses in the carbonates, 0.5–1 mg were used. Organic matter was removed following standard procedures (Cerling et al., 1997) and the samples were then acidified with phosphoric acid (supersaturated: 103 %), producing CO_2 analyzed for isotopic content using a ThermoFisher Kiel IV carbonate device connects to Thermo Scientific Delta V+ stable isotope ratio Mass Spectrometer (AETE-ISO platform, OSU-OREME, University of Montpellier). The within-run precision (±1 σ) of these analyses as determined by the replicate analyses of NBS 18 and AIEA-603 was less than ± 0.2 ‰ for $\delta^{13}C$ and ±0.3 ‰ for $\delta^{18}O$ (n = 5–6 respectively). Results are expressed as ratio (‰) to the Vienna-Pee Dee Belemnite (VPDB) standard as follows:

$$\delta = 1000 \times \left(\frac{R_{sample}}{R_{standard}} - 1\right)$$

where R_{sample} refer to the ratio of $\frac{^{13}C}{^{12}C}$ and $\frac{^{18}O}{^{16}O}$ of the sample and $R_{standard}$ to the VPDB standard.

The $\delta^{13}C_{CO3,\ enamel}$ is converted into the $\delta^{13}C_{diet}$ as detailed below.$\delta^{13}C_{diet} = \delta^{13}C_{CO3,\ enamel} - \varepsilon^{*}_{diet-bioapatite} - corr$ where $\varepsilon^{*}_{diet-bioapatite} = e^{2.42+0.032\times ln(bodymass)}$ (Tejada-Lara et al., 2018) and corr is the correction factor for the variation of $\delta^{13}C_{CO2}$ of the atmosphere. Post 1930, the values of $\delta^{13}C_{CO2}$ are −8 ‰ (Zachos et al., 2001). During the Late Pleistocene, the reconstructed values of $\delta^{13}C_{CO2}$ based on benthic foraminifera (Tipple et al., 2010) are around −7 ‰ corresponding to a correction factor of 1.

The $\delta^{13}C_{diet}$ is used to estimate the mean annual precipitation (MAP). We used the equation of Rey et al. (2013): $MAP = 10^{0.092\times\Delta^{13}C_{leaf}+1.148} - 300$ where $\Delta^{13}C_{leaf} = \frac{\delta^{13}C_{atm}-\delta^{13}C_{diet}}{1+\frac{\delta^{13}C_{diet}}{1000}}$.

Regarding oxygen content, the $\delta^{18}O_{CO3(V\text{-}PDB)}$ can be converted into the $\delta^{18}O_{CO3(V\text{-}SMOW)}$ following the equation from Coplen et al. (1983): $\delta^{18}O_{V-SMOW} = 1.03091 \times \delta^{18}O_{V-PDB} + 30.91$.

The $\delta^{18}O_{CO3(V\text{-}SMOW)}$ was used to infer the $\delta^{18}O_{precipitation}$ and the mean annual temperature (MAT). Regarding rhinocerotids, no dedicated reliable equation to estimate the $\delta^{18}O_{precipitation}$ based on the $\delta^{18}O_{enamel}$ is available in the literature. Hence, we decided to use an equation designed for elephants (Ayliffe et al., 1992), as body mass and metabolism of rhinocerotids should be closer to that of elephants than of ruminants or horses (specialized grazers, domesticated): $\delta^{18}O_{PO4} = 0.94 \times \delta^{18}O_{precipitation} + 23.3$.

As the $\delta^{18}O$ used is that of phosphates, we converted our results into $\delta^{18}O$ of carbonates according to the phosphates-carbonates relation from Lécuyer et al. (2010): $\delta^{18}O_{PO4} = 0.96 \times \delta^{18}O_{CO3} - 8.05$.

This results in the following relation: $\delta^{18}O_{precipitation} = 1.02 \times \delta^{18}O_{CO3} - 33.3$.

Eventually, for the MAT we followed the equation for Central Europe proposed by Skrzypek et al. (2011):

$$MAT = 1.41 \times \delta^{18}O_{precipitation} + 23.63.$$

2.7. Statistics and figures

All statistics were conducted in R (R Core Team, 2021: v. 4.1.2) equipped with the package tidyr (Wickham and Henry, 2020), MASS (Ripley et al., 2013) and mvnormtest (Jarek, 2012). Following the recent statement of the American Statistical Association (ASA) on p-values (Wasserstein and Lazar, 2016), we tried to avoid classical thresholds of "statistical significant" and to give exact values instead. Figures were done using R packages ggplot2 (Wickham, 2016), ggtern (Hamilton and Ferry, 2018), cowplot (Wilke, 2020), as well as Inkscape (v. 1.0.1).

In the case of small samples (<5) and ordinal categorical variables (mesowear score), we used non-parametric tests (Kruskal-Wallis for median comparison, Spearmann rho for correlation testing). When possible, we used parametric tests (MANOVA, ANOVA and post hoc tests) after a Box-Cox transformation to obtain a normal distribution of the variables.

3. Results

3.1. Paleobiology: minimal number of individual (MNI), age structure, mortality, and body mass

The MNI of *C. antiquitatis* at the studied localities was estimated based on dental remains. The MNI was mostly below 5, but ranging from 1 at Gönnersdorf to 22 at Goyet's third cave (Table 3). Indeed, the number of teeth available was limited at several localities (<50; Table 1), but some yielded more abundant material and MNI, notably Knochenkies Bottrop (MNI = 18), Hofstade (14), Caverne Marie-Jeanne (11), North Sea (21), Kent's cavern (14), and Goyet's third cave (22). At these localities, mortality profiles were constructed (Fig. 2). When corrected for the duration of the age classes, the profiles were all L-shaped with a major peak at age class I, corresponding to the period shortly after birth, except at Hofstade. For the latter, there is a global peak during early life (age classes II, IV, V, and VII). In addition to this main peak around age class I, other peaks of lesser amplitude are observed on the different mortality profiles, notably around age classes II, IV and VII (Fig. 2).

The age structure of the studied *C. antiquitatis* samples varied greatly depending on the locality considered (Chi2, X-squared = 59.743, df = 13, p-value = 5.84×10^{-8}; Fig. 3). However, most samples fall within the range displayed in extant rhinoceros populations, with about 15–25 % juveniles, 13–20 % subadults, and 60–80 % adults. On the other hand, a taphonomical or sampling bias might be suspected at some localities, notably Brixham cave (0 % of juveniles), North Sea (6.92 % of juveniles), Bottrop (7.65 % of juveniles), Caverne Marie-Jeanne (28.14 % of juveniles), and Irpfelhöhle (32.14 % of juveniles).

Coelodonta antiquitatis was a large sized rhinoceros, with median values of all proxies estimated between 1850 kg at Caverne Marie-Jeanne and 2955 kg at Bocksteinhöhle (Table 3). We did not detect trends in body mass due to geographical provenance (Kruskal-Wallis chi-squared = 0.21857, df = 2, p-value = 0.8965). When the localities are ordered chronologically, the variations of the body mass are sinusoidal, mostly fluctuating between 1850 and 2450 kg (Fig. 4).

Interestingly, there is a correlation between the variations of body mass and that of hypoplasia prevalence (Spearmann rho = 0.5549451, S = 162, p-value = 0.05253). The main uncoupling in this relationship is observed for Kent's cavern, and to a lesser extent for North Sea and Jaurens (Fig. 4). There is however no correlation between body mass and mesowear score (Spearman rho = −0.2841417, S = 584.28, p-value = 0.3249), nor with any microwear parameters (Spearman rho, p-values > 0.2).

3.2. Prevalence of enamel hypoplasia

The overall prevalence of hypoplasia in our sample (all localities merged) was high, with about 20 % of the teeth studied bearing at least one defect (328/1637). There are however great disparities depending on the loci (Kruskal-Wallis chi-squared = 205.72, df = 19, p-value < 2.2e-16) and localities (Kruskal-Wallis chi-squared = 37.273, df = 13, p-value = 0.0003754), as visible in Fig. 5. The highest prevalences are found at Bocksteinhöhle (8/17; 47.06 %), Weinberghöhlen (12/33; 36.36 %), and Göpfelsteinhöhle (8/27, 29.63 %), whereas the lowest

Table 3
Summary of the main results of the multi-proxy approach on *Coelodonta antiquitatis* by locality.

	MNI	Body Mass (kg)	Hypoplasia (%)	δ13CCO3, enamel (‰ V-PDB)	δ18OCO3, enamel (‰ V-PDB)	Mesowear (M1 and M2)
Gönnersdorf	1	–	–	−9.75	−8.17	–
Brixham cave	2	2220	18.75	–	–	5
Jaurens	5	2200	9.38	–	–	5.5
Goyet	22	2390	25.22	−9.56	−6.60	6
Kent's cavern	14	2440	16.67	–	–	6
Ofnethöhle	4	1950	21.28	−10.05	−9.08	5.5
Vogelherdhöhle	2	–	26.67	−11.06	−9.38	6
Bocksteinhöhle	3	2955	47.06	−11.61	−9.12	5
North Sea	21	2010	17.8861788617886	–	–	6
Marie-Jeanne	11	1850	19.68	–	–	6
Weinberghöhlen bei Mauern	6	2230	36.36	–	–	5
Göpfelsteinhöhle	5	2360	29.63	−9.67	−8.90	6
Irpfelhöhle	3	1920	7.41	–	–	6
Hofstade	14	1980	11.67	–	–	6
Knochenkies Bottrop	18	2345	22.27	–	–	6

Mean values at the locality for stables isotopes and median values for body mass (all proxies) and mesowear. MNI - minimal number of individuals, VPDB - Vienna-Pee Dee Belemnite standard.

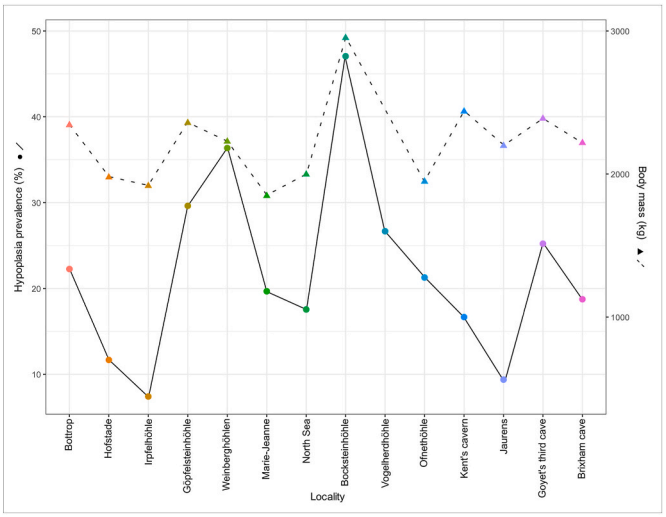

Fig. 4. Co-variation of body mass (dashed line) and hypoplasia prevalence (full line) in *Coelodonta antiquitatis*.
Localities ordered chronologically from oldest (left) to youngest (right). Color code by localities as in previous figures.

ones are at Irpfelhöhle (2/27; 7.41 %), Jaurens (6/64; 9.38 %), and Hofstade (14/120; 11.67 %). Despite these locality differences, the geographical provenance (Northern Europe or Western Europe) did not impact greatly hypoplasia prevalence (Kruskal-Wallis chi-squared = 0.36836, df = 1, p-value = 0.5439). Concerning loci, the most affected ones are D4 (42/72; 58.33 %), m3 (59/143; 41.26 %), and M3 (52/130; 40 %), while the least affected ones are d1 (0/7), d2 (0/21), and p2 (1/59; 1.69 %). In general, milk molars are rarely affected (0–6.5 %) except from d4/D4.

3.3. Dental wear

As the mesowear was studied in only one species, the changes in hypsodonty should be minor and should not impact greatly the mesowear. The hypsodonty index could be estimated only for a few localities (Caverne Marie-Jeanne, North Sea, Kent's cavern, Goyet's third cave, Jaurens, and Brixham cave), but was between 2.12 and 2.43, indicating mesodont teeth. The mesowear score is always very high, with median values between 5 and 6 (Table 3; Fig. 6). This suggests very abrasive dietary preferences consistent with grazing. There were however slight variations through time, but no clear differences between localities (Kruskal-Wallis chi-squared = 18.434, df = 13, p-value = 0.1417). We also studied mesowear on milk cheek teeth to identify changes in the diet between juveniles and adults. We found lower values compared to their permanent counterparts (Kruskal-Wallis chi-squared = 76.613, df = 1, p-value <2.2e-16).

Regarding dental microwear texture (DMT), we noted more spatio-temporal variations (Fig. 7). The DMT signatures were different by locality (MANOVA, p-value = 0.029) and to a lesser extent by facet (MANOVA, p-value = 0.097). We conducted ANOVAs for each DMT parameter (Asfc, Str, HAsfc9 and HAsfc81) to precise the differences. There was only a marked influence of facet (p-value = 0.025) and locality (p-value = 2.5×10^{-4}) on Asfc. Tuckey's post hoc did not highlight specific pairs of localities with significant Asfc differences (see Supplementary A).

The variations of anisotropy (inverse of Str) and complexity (Asfc) display a sinusoidal evolution on both facets, although less clear on the shearing one (Fig. 7). Moreover, the geographical provenance also impacted the variations of Afsc (Kruskal-Wallis chi-squared = 17.913, df = 2, p-value = 0.0001289). The mean values of Str at the different localities were above 0.5 on both facet, except at Hofstade (grinding: 0.45), Kent (grinding: 0.48), and Marie-Jeanne (shearing: 0.38). In extant species (rhinoceros and tapirs), such medium to high Str values typically suggest mixed-feeding or browsing habits (see Fig. 4 in Supplementary B). As to be expected, the specimens with low dietary abrasivity (high Str: Weinberghöhlen, Bocksteinhöhle, and Ofnethöhle) also have lower mesowear scores (Table 3; Fig. 6). The values of Asfc were mostly below 2, except on the shearing facet at Ofnethöhle (2.47), suggesting a rather soft diet. There was a positive correlation between Afsc and both Hasfc studied here (H9: Spearman rho = 0.1520718, S = 496272, p-value = 0.0615; H81: Spearman rho = 0.1736036, S = 483670, p-value = 0.03256) indicating a greater diversity in the diet when harder objects were consumed.

3.4. Stable isotopes

The analyses of the isotopic content (carbon and oxygen) in the carbonates of the rhinocerotids' enamel revealed marked differences between the studied localities (Table 3; Fig. 8). All specimens were in the range of C_3 feeding, with values of the $\delta^{13}C_{diet}$ comprised between −24.11 and −27.34 ‰ (Fig. 8). *Coelodonta antiquitatis* from Bocksteinhöhle had the lowest values (≤−26.9 ‰), while the highest values were observed at Goyet's third cave (>−24 ‰), suggesting more open arid conditions at the latter. Regarding the oxygen content, values of the $\delta^{18}O_{CO3,\ SMOW}$ ranged from 19.91 to 25.55 ‰ (Fig. 8). Most specimens studied had values lower than 22 ‰, except those from Goyet for which

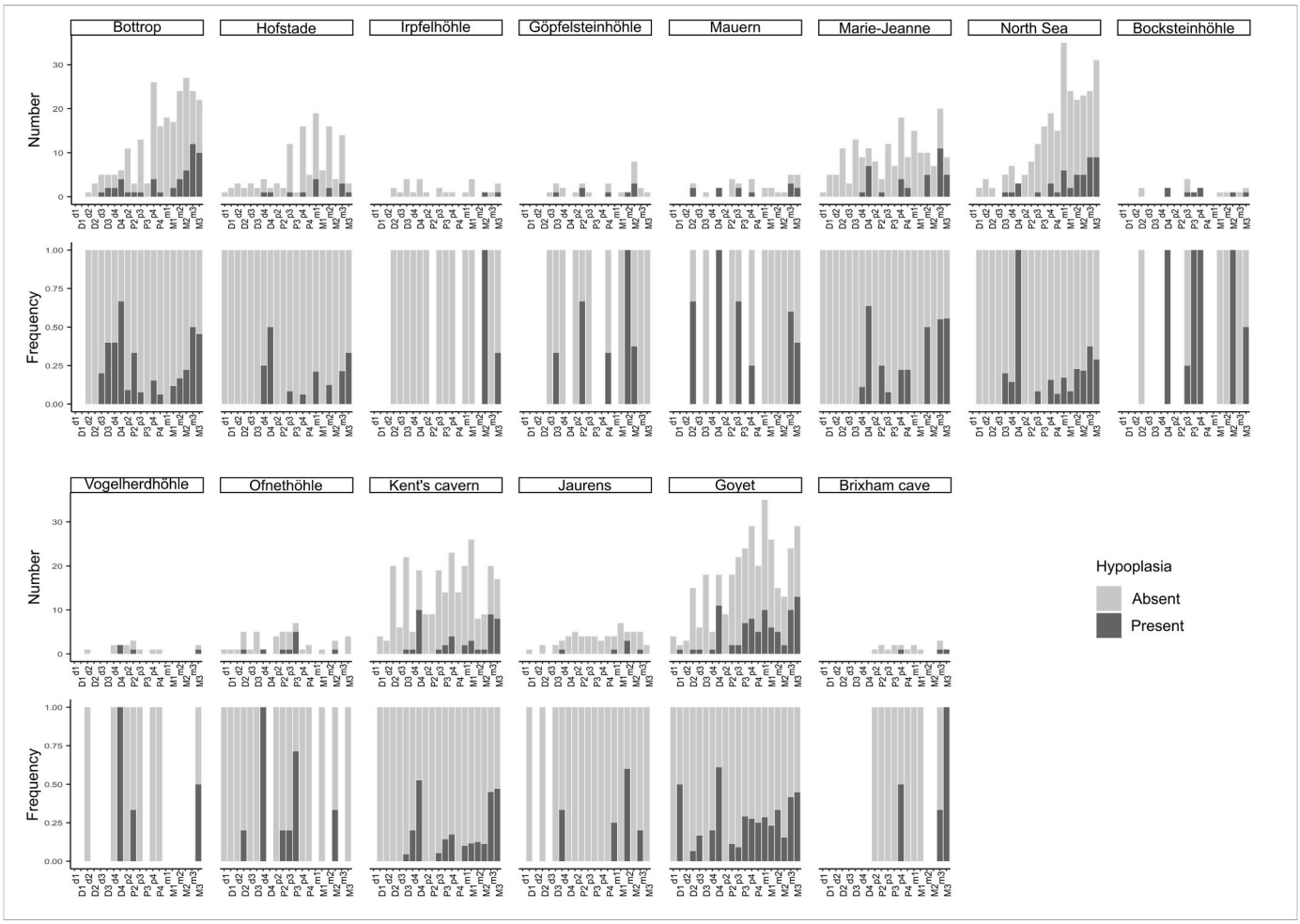

Fig. 5. Number and frequency of hypoplastic teeth in *Coelodonta antiquitatis* by locus and locality.

all specimens had values above 23 ‰, indicating higher temperatures at the latter.

These isotopic analyses allow for some paleoenvironmental insights (Table 4). These insights must however be taken with caution, as the sample is restricted to *C. antiquitatis* and limited in specimens. The MATs reconstructed are between 6.8 °C at Bocksteinhöhle and 11.4 °C at Goyet. The MAPs range from 403 mm/year at Goyet to 826 mm/year at Bocksteinhöhle.

In order to investigate seasonality, teeth of four localities were serially sampled (Göpfelsteinhöhle, Ofnethöhle, Goyet's third cave, Gönnersdorf). For most specimens, intra-specific variation was low to moderate (0.5–2 ‰) for both $\delta^{13}C_{CO3}$ and $\delta^{18}O_{CO3}$. Sinusoidal patterns were observed for most specimens (see Supplementary B), except those from Gönnersdorf, as the tooth fragments were too small to get enough samples for a sinusoidal pattern to show. The co-variation of $\delta^{13}C_{CO3}$ and $\delta^{18}O_{CO3}$ values was tested, as it indicates a consistent influence of seasonal precipitation on the plants consumed. Such a correlation was found at Göpfelsteinhöhle (Spearman rho = −0.7903644, S = 150.39, p-value = 0.01956) and Gönnersdorf (Spearman rho = 0.6107894, S = 32.694, p-value = 0.1077), but not at Ofnethöhle (Spearman rho = −0.1431905, S = 251.5, p-value = 0.6745), nor at Goyet (Spearman rho = −0.1911036, S = 12697, p-value = 0.2375).

4. Discussion

4.1. Age structure, stress susceptibility and body mass

The age structures of the *C. antiquitatis* samples are in the range of that of extant rhinoceros populations for most localities (Fig. 3). Some localities are, however, outside of this range, mostly due to the fraction of juveniles. There is an under-representation of juveniles at Brixham cave (0 % of juveniles), North Sea (6.92 % of juveniles), and Bottrop (7.65 % of juveniles). The under-representation of juveniles at fossil sites might be due to the more fragile nature of juvenile remains (more prone to weathering or displacement), to predation or to scavenging (Germonpré, 1993). Predation and bite marks from hyena are reported at Bottrop on woolly rhinoceros remains (Diedrich, 2012), while weathering or displacement is more likely at North Sea, as the specimens were retrieved during dragging of the sea floor (Geel van et al., 2019). Moreover, a total absence of juveniles similarly to Brixham cave was already observed and discussed (taphonomic bias, displacement) for *Brachypotherium brachypus* during the late Early Miocene at Béon 1 in France (Hullot and Antoine, 2020) and *Aphelops malacorhinus* during the Late Miocene at Love Bone Bed in the US (Mihlbachler, 2003). On the other hand, juveniles are over represented at Marie-Jeanne (28.14 % of juveniles), and Irpfelhöhle (32.14 % of juveniles). Such a pattern has already been observed to a greater extent (33–92 % of juveniles) for *Rhinoceros* and *Dicerorhinus* at several Pleistocene sites in Asia (Nam Lot, Coc Muoi, Sibrambang, Punung, Tam Hang, and Duoi U'Oi) and *C. antiquitatis* at Fouvent (Bacon et al., 2008, 2011, 2015, 2018; Antoine, 2012; Fourvel et al., 2015). This often indicates dens of scavengers (hyenas, porcupines; Fourvel et al., 2015; Bacon et al., 2018).

The age structure of *C. antiquitatis* was previously inferred at Bottrop, Hofstade, and Goyet. At Bottrop, Diedrich (2012) reported about 5 % of calves in *C. antiquitatis*' remains (cranial and post cranial), which is relatively similar to our estimates on dental material (7.65 %; Fig. 3). At

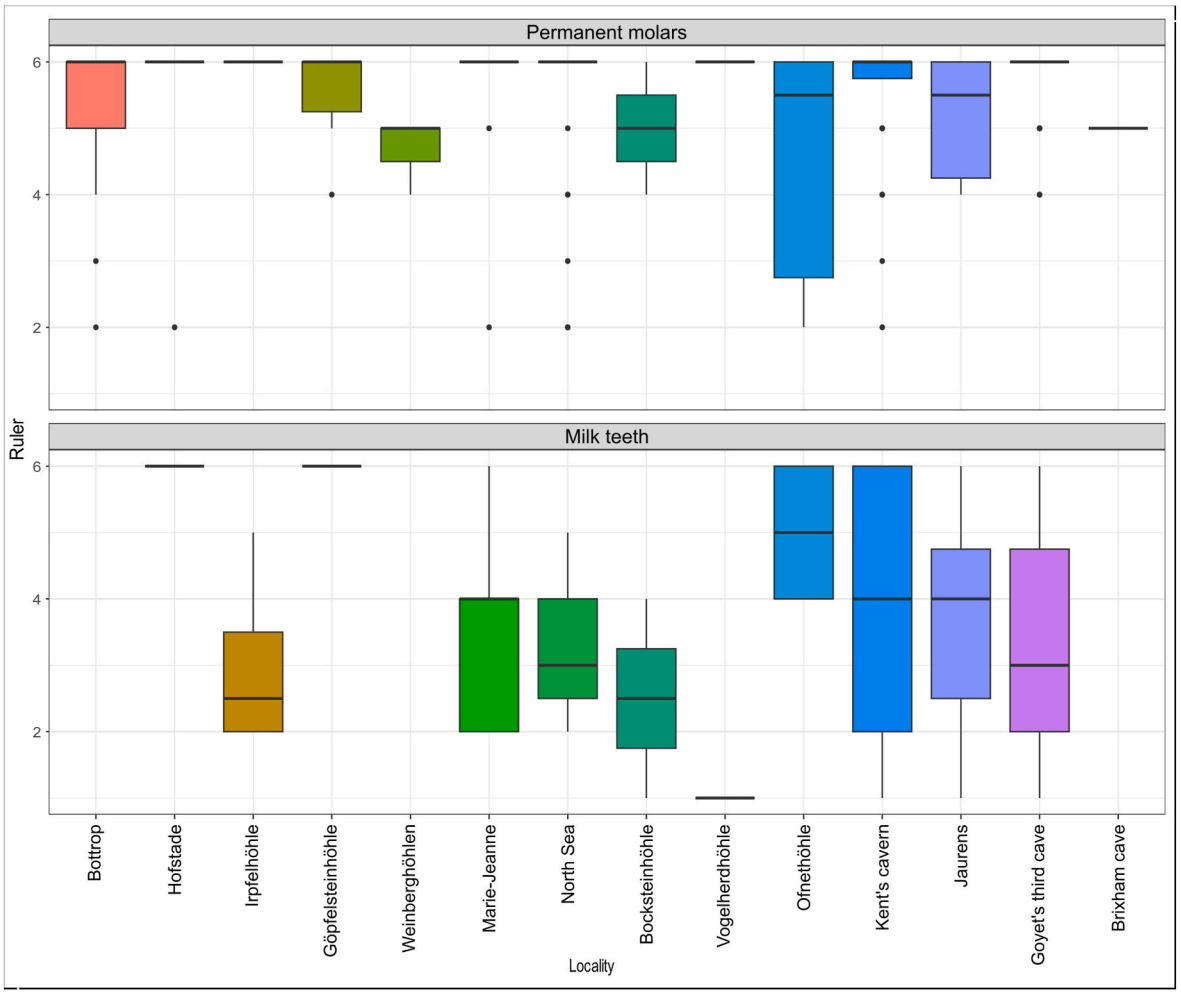

Fig. 6. Evolution of the mesowear score of *Coelodonta antiquitatis* across the studied localities (ordered chronologically). Color code by locality as in previous figures.

Hofstade, our estimates are slightly higher in term of juveniles and subadults compared to that of Germonpré (1993; juveniles: 15.3 vs. 9.1 % and subadults: 17.6 vs. 13.6 %), but she only studied the mandibles, while here we also considered isolated teeth. A previous study (Hullot and Antoine, 2020) pinpointed that considering only associated or isolated teeth can change the age structure estimated, which might explain the discrepancies noted here. Eventually, at Goyet, Comeyne (2013) reported a dominance of subadults in the sample (about 75 %) and an under-representation of adults, but only the material from the third horizon was considered corresponding to 24 teeth.

The mortality curves were L-shaped at Knochenkies Bottrop, Caverne Marie-Jeanne, North Sea, Kent's cavern, Jaurens, and Goyet's third cave (Fig. 2). This shape is typical of idealized attritional mortality profile of stable populations (Mihlbachler, 2003), which suggests that the studied samples were large enough to represent living populations. The profile was however different at Hofstade and Ofnethöhle, indicating potential sampling and/or taphonomical biases. At Hofstade, most teeth were from mandibles (i.e., associated teeth), and hence few individuals, which has been shown to affect mortality curves results (Hullot and Antoine, 2020).

Regarding stress susceptibility, the most affected locus varies depending on localities, but D4 is the most common (58.33 % affected in the whole dataset), suggesting early-life stresses around birth. High stresses around birth are also consistent with the peak in mortality observed in the mortality profiles for age classes I and II (Fig. 2), that correspond to 1.5–4 months old individuals in the extant white rhinoceros (Hillman-Smith et al., 1986). This increased susceptibility period close to birth has previously been reported in other rhinocerotid species from the Miocene (Hullot et al., 2021, 2023). Such a finding is not surprising as birth is known to be a stressful time for most mammals (Upex and Dobney, 2012), especially under the harsh environmental conditions of the Würm/Weichselian glaciation.

Second molars (22.33 % affected in the whole dataset) and fourth premolars (16.45 %) are also commonly bearing hypoplasia defects, which indicates stresses from weaning to cow-calf separation (Mead, 1999; Niven et al., 2004). Interestingly, the mortality profiles of *C. antiquitatis* at some the studied localities display peaks in mortality at age class IV and VII (Fig. 2). In Hullot and Antoine (2020), weaning was correlated with age classes V-VI (1.5–4 years old in the extant white rhinoceros), but inter-specific variations or a delayed weaning might explain such differences. Delayed weaning has been observed in modern elephants under harsh conditions, and have already been hypothesized for *Mammuthus primigenius* (woolly mammoth) during glacial times (Metcalfe et al., 2010).

Eventually, third molars also had great hypoplasia prevalences (40.66 % affected in the whole dataset). Hypoplasia on third molars have already been correlated with environmental stress in several taxa (Franz-Odendaal et al., 2003; Skinner and Pruetz, 2012; Upex and Dobney, 2012). Interestingly, particularly cold and harsh conditions can be inferred at Bottrop, Hofstade, and Brixham cave, as they date to particularly cold stadials (OIS4 for the first two, and OIS2 for Brixham; Lisiecki and Raymo, 2005; Genty et al., 2010; Skrzypek et al., 2011).

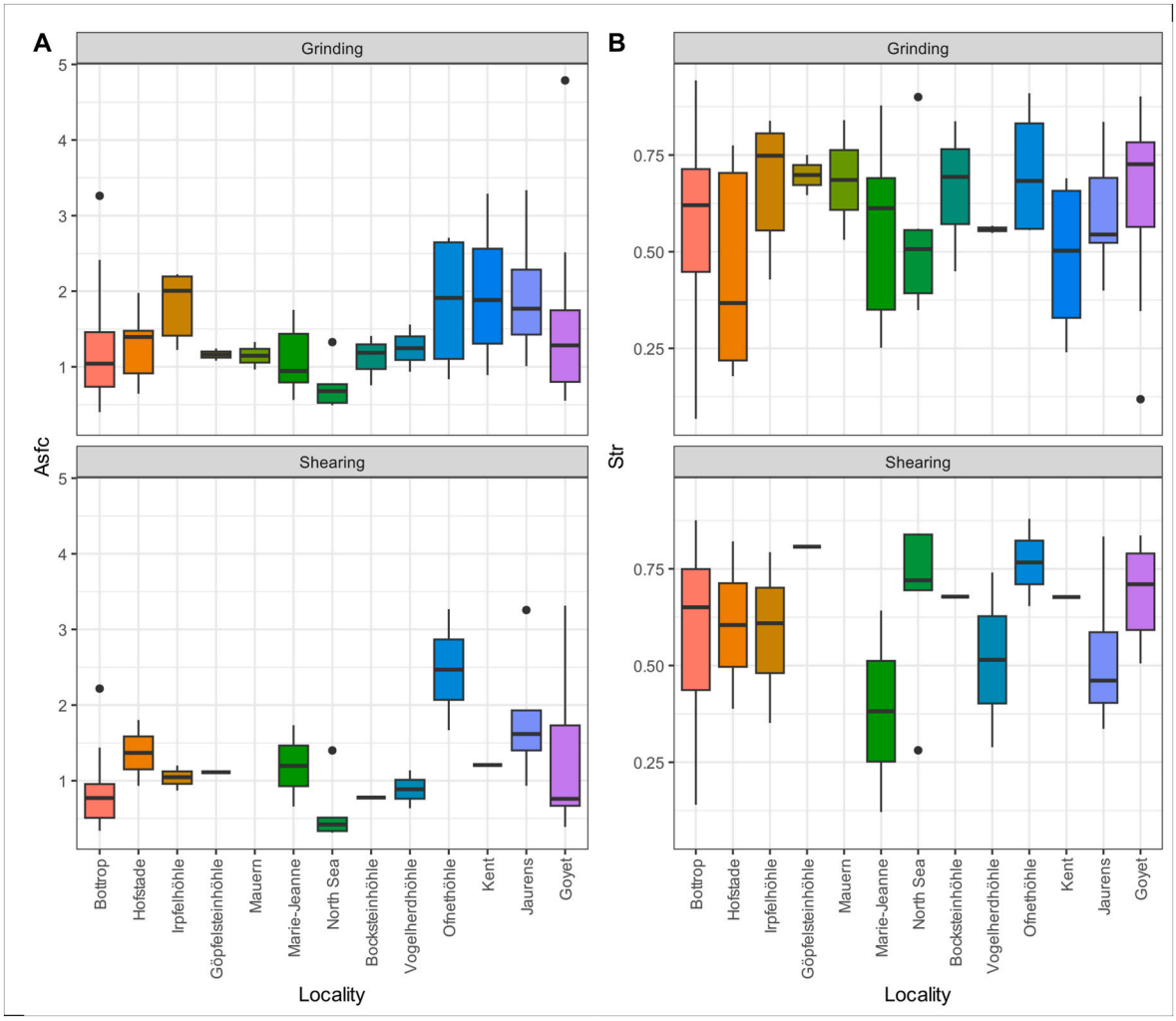

Fig. 7. Evolution of the DMT signature of *Coelodonta antiquitatis* at the studied localities.
A – Complexity (Asfc), B – Anisotropy (Str). Localities ordered chronologically and colored as in previous figures.

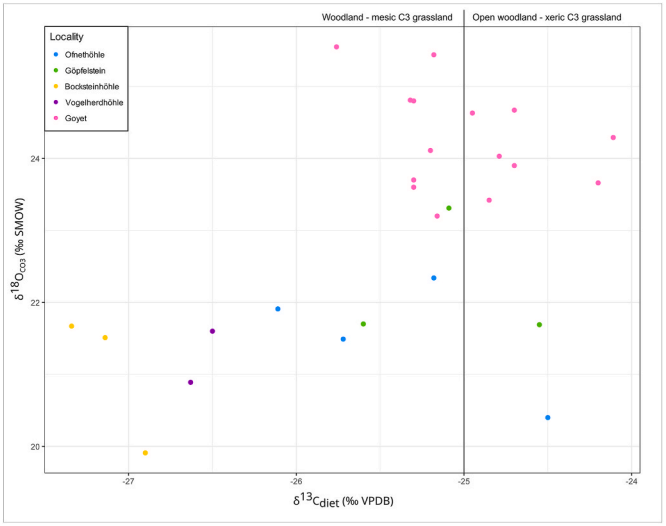

Fig. 8. Stable isotopic signal (carbon and oxygen) of Coelodonta antiquitatis. Color code by locality as detailed in the figure. Biotopes' threshold according to Domingo et al. (2013).

Table 4
Reconstruction of the mean annual temperature (MAT) and precipitation (MAP) at the studied localities based on the isotopic content of the enamel carbonates of *Coelodonta antiquitatis*.

	MAT (°C)	MAP (mm/year)
Gönnersdorf	8.92	417.50
Ofnethöhle	7.54	470.24
Goyet	11.44	403.44
Vogelherdhöhle	7.13	693.45
Bocksteinhöhle	6.82	826.24
Göpfelsteinhöhle	8.55	417.99

Germonpré (1993) has already inferred recurrent severe cold-dry periods causing catastrophic mortalities of rhinoceros at Hofstade I, based on the mortality profile of the species. However, most localities studied here (Irpfelhöhle, Göpfelsteinhöhle, Weinberghöhlen bei Mauern, Caverne Marie-Jeanne, North Sea, Bocksteinhöhle) probably date to a warmer period of the OIS3 (~59-41 kya; Skrzypek et al., 2011).

The body mass estimates for *C. antiquitatis* at the studied localities ranged from 1850 to 2955 kg. These values are in the range of what has been previously reported for the species based on various proxies and at various localities (2900 kg in Stuart, 1991; 1.5 to 2 t in Boeskorov, 2012; 1038–2935 kg in Saarinen et al., 2016). These estimates are also close to what is observed for the white rhinoceros (*Ceratotherium simum*) today (Dinerstein, 2011). Interestingly, the morphology of both species have

often been compared and several similarities have been pinpointed (high crowned teeth, elongated head with a low carriage; Garutt, 1994; Uzunidis et al., 2022), leading to assumptions of a similar ecology (open habitat, strict grazer). However, this shortcut is not supported and the paleoecological preferences of *C. antiquitatis* were more diverse, as detailed thereafter.

4.2. Insights from dental wear

Our results on paleoecological preferences (dental wear and stable isotopy), suggest great spatio-temporal variations, indicating a certain plasticity in the food sources of *C. antiquitatis*. The mesowear scores are very high for *C. antiquitatis* at all localities (Table 3; Fig. 6), pointing towards dominant grazing habits consistent with the morphology (high crowned teeth with secondary cement) and previous finding from the literature (Boeskorov et al., 2011; Stuart and Lister, 2012; Rivals and Lister, 2016; Geel van et al., 2019; Stefaniak et al., 2020). A strict grazing behavior similar to that of the extant white rhinoceros is however unlikely, as the spatio-temporal variations in dental wear and carbon content of the enamel suggest a greater dietary diversity (Fig. 6; Fig. 7; Fig. 8).

Such plasticity in *C. antiquitatis* has already been reported in previous works using various proxies. For instance, Guérin (1980) noted that the hypsodonty index of *C. antiquitatis* was lower than that of the extant strict grazer *Ceratotherium simum*, and suggested a less monotypic diet for *C. antiquitatis*. Similarly, a mesowear approach on lower teeth suggested that *C. antiquitatis* had intermediate dietary preferences between that of the strict grazer *C. simum* and that of the variable grazer *Rhinoceros unicornis* (Hernesniemi et al., 2011). Eventually, several studies have highlighted the consumption of browsing resources at least periodically, such as forbs (non-graminoid herbaceous vascular plants) and mosses (ancient DNA metabarcoding: Willerslev et al., 2014), woody components (mesowear: Saarinen et al., 2016; pollen and spores: Geel van et al., 2019), and Cyperaceae fruits (*Carex*), aquatic plants, and seeds or leaves of *Betula* and *Plantago* (plants macro remains: Stefaniak et al., 2020). All these suggests that *C. antiquitatis* was a variable grazer with seasonal, as well as spatio-temporal differences in its dietary preferences. Such a diet is closer to that of *R. unicornis* rather than that of *C. simum* (Hullot et al., 2019).

The mesowear scores of deciduous teeth were lower than that of permanent teeth (Fig. 6), indicating less abrasive food items in the diet of the juveniles. This lower abrasive load could result from pre-weaning habits (Bullington, 1991; Hamilton and Barclay, 1998), allowing for a longer lifespan of the thinner and softer enamel band in deciduous teeth (Carvalho et al., 2017), and keeping small competition for resources with adults (Polis, 1984; Jeglinski et al., 2013).

We found no correlation between body mass and mesowear nor microwear in the sample studied here. Previous studies already reported an absence of correlation between body mass and diet for various herbivores, including *C. antiquitatis* (Steuer et al., 2014; Saarinen et al., 2016; Orlandi-Oliveras et al., 2022). Instead of diet, body size might correlate better with habitat openness. Indeed, a large size confers advantages in open environments, especially challenging ones such as the tundra-steppe of the Würmian/Weichselian Eurasia, notably an increased resistance to seasonal shortages of food and water (Peters, 1983; Clauss et al., 2003) and a better energy-efficient locomotion helping for predator avoidance (Peters, 1983). At first glance, an increased resistance of large species to seasonality is contradictory with our results, as hypoplasia prevalence and body mass co-variate (Fig. 4), suggesting a greater stress susceptibility of *C. antiquitatis* at localities with greater body mass. However, for a stress (or combination of stresses) to be recorded as a hypoplastic defect, the individual must survive. Thus, a large size probably does not prevent stress such as seasonal shortages of food and water to affect the metabolism, but may rather increase resilience.

4.3. Insights from stable isotopy

Our results regarding the carbon content of *C. antiquitatis* enamel suggest a pure C_3 environment and diet (Fig. 8), consistent with the knowledge that C_4 grasses were never dominant in Europe, contrary to other regions of the world (Strömberg, 2011; Saarinen et al., 2020). Other isotopic analyses on European Pleistocene rhinoceroses (*Stephanorhinus*, *Coelodonta*) also suggest a C_3 environment (Pushkina et al., 2014; Stefaniak et al., 2020; Rey-Iglesia et al., 2021; Zanazzi et al., 2022). Regarding the range of values, our results on $\delta^{13}C_{CO3,\ enamel}$ (−11.8 to −8.7‰) are similar to that reported by Stefaniak et al. (2020) for *C. antiquitatis* from various studies in Western and Central Europe from Middle to Late Pleistocene (−13 to −9 ‰). In the same work, the authors did not find significant differences in $\delta^{13}C_{CO3,\ enamel}$ with respect to chronology (except between late Middle Pleistocene and late Late Pleistocene) and to geographic regions (Stefaniak et al., 2020). They also suggest low dietary flexibility for *C. antiquitatis* contrary to our findings and to the literature (Rey-Iglesia et al., 2021). However, this interpretation is based on a more restricted dataset and on the isotopic content only, without considering attritional and abrasional aspects of mastication.

Regarding $\delta^{18}O_{CO3,\ enamel}$ there are greater variations than compared to $\delta^{13}C_{CO3,\ enamel}$ in both our dataset (−10.67 to −5.2 ‰) and the one reported by Stefaniak et al. (2020; −13.98 to −6.93 ‰) suggesting spatio-temporal variation of the climatic conditions within Europe. However, no significant trend by chronology nor region is detectable, which could suggest a relatively strict climatic niche for *C. antiquitatis*. Indeed, despite spatio-temporal variations in the diet of *C. antiquitatis*, its overall climatic niche is rather restricted to the cold conditions of the tundra-steppe habitat (Stefaniak et al., 2020; Rey-Iglesia et al., 2021). A strict climatic niche might explain the persistence of *C. antiquitatis* only in restricted zones (Siberia) during the latest Pleistocene deglaciation and its extinction associated with the disappearance of its habitat, fragmentation of populations, and climatic instability (Kuzmin, 2010; Stuart and Lister, 2012; Rey-Iglesia et al., 2021).

Interestingly, the isotopic results also give some insights into the local environmental conditions. Our results suggest substantial spatio-temporal variation of MAT and MAP, as previously reported in Central Europe (Skrzypek et al., 2011). The estimated MATs, between 6.5 and 11.5 °C (Table 4), are rather cold and comparable to today's MATs at high latitudes (e.g., Toronto: 8.7 °C, Stockholm: 7.3 °C; https://en.climate-data.org). They seem however relatively mild for glacial times in Central and Northern Europe. Indeed, previous works reported MATs between −10 and 0 °C in Belgium and the Netherlands (Germonpré, 1993; Vandenberghe and Pissart, 1993) during the Pleniglacial (73–12.5 kya) and the Late Glacial (12.5–10 kya), and around 0 during interstadials and −10 °C during stadials in Northern Germany (Shao et al., 2021). Most localities studied here date from the Early Weichselian (OIS5; 115 to 73 kya) or from the OIS3 (57-29 kya), both periods corresponding to interstadials (Germonpré and Sablin, 2001; Wohlfarth, 2013). During these intervals, reported MATs in Central Europe were estimated around 6.8 °C (115–74 kya; OIS5) and 6.3 °C (59 and 41 kya; OIS3) respectively (Skrzypek et al., 2011). As stated above, several localities investigated here probably date to the second warmer interval, including Göpfelsteinhöhle and Bocksteinhöhle for which isotopic content was studied. This could explain the mild MATs reconstructed there.

Nevertheless, several problems exist regarding the precise estimation of MATs based on large herbivores (see discussion in Zanazzi et al., 2022), notably when using only one taxon and a restricted sample. When compared to the results from other associated taxa (*Equus caballus*, *Mammuthus primigenius*, and *Megaloceros giganteus*), MAT estimates based on *C. antiquitatis* enamel were consistently higher (6.82 vs. 2.76 °C at Bocksteinhöhle and 7.13 vs. 2.86 °C at Vogelherdhöhle; Pushkina et al., 2014). This might be due to absence of a specific robust equation for rhinoceros to estimate $\delta^{18}O_{precipitation}$. Indeed, the one from Tütken et al. (2006) was only preliminary and yielded aberrant MAT estimates,

that are 5–6 °C higher than the ones estimated with the equations for horses (Sánchez Chillón et al., 1994), deer (D'Angela and Longinelli, 1990), bison (Bernard et al., 2009), or elephants (Ayliffe et al., 1992; see Supplementary A).

Regarding precipitation, our estimates are quite low (< 500 mm/year) for most localities studied (Table 4), consistent with the tundra-steppe polar conditions of the Late Pleistocene. Indeed rain- and snowfall are generally limited in present day closest biomes (tundra, taïga), due to the low vapor pressure of water under these conditions (Yurtsev, 2001). Previous estimates of MAPs in Northern Germany were around 500 mm per year during the Early Weichselian (Kühl et al., 2007), similar to our values although our localities are younger. Likewise, the estimates at Caverne Marie-Jeanne (isotopes not studied here) fall in a similar range, between 500 and 1000 mm/year depending on the level considered and hence the age (Blain et al., 2019)

With respect to seasonality, the moderate intra-tooth variability in enamel carbon and oxygen content (0.5–2 ‰) likely indicates moderate seasonal contrasts in temperature and precipitation. This result could be partly explained by isotope damping, which attenuates the variations of $\delta^{18}O$ along the crown during the maturation of the enamel (Zazzo et al., 2005; Martin et al., 2008). Indeed, similar ranges of variability have been reported for $\delta^{18}O$ of various rhinocerotid species from different periods and regions for instance: ~2‰ in *Stephanorhinus* and *Coelodonta* from the Middle Pleistocene of Italy (Zanazzi et al., 2022), 1–1.9‰ in modern and Miocene rhinocerotids under tropical conditions (MacFadden and Higgins, 2004; Martin et al., 2008; Zin-Maung--Maung-Thein et al., 2011), 1.1–1.3‰ from the Miocene rhinocerotids of Southeastern United States (DeSantis and Wallace, 2008). Some datasets display slightly higher variations: 2.0–2.5‰ for Miocene-Pliocene rhinoceroses from continental China (Zhang et al., 2012; Ciner et al., 2015; Biasatti et al., 2018), and 2.2–3.9‰ for Eocene, Oligocene, and Miocene rhinocerotids from continental North America (Zanazzi and Kohn, 2008; Zanazzi et al., 2015; Harris et al., 2020). Moreover, a previous study revealed that the $\delta^{18}O$ in extant rhinoceros' enamel seems not to be very sensitive to changes in aridity (Levin et al., 2006), which would suggest that rhinocerotids might not be the best taxa to track seasonality through oxygen content. Besides this metabolic buffering, other parameters might explain the moderate seasonality inferred. For instance, as discussed above, most localities studied date to a milder interval of the OIS3 (59 and 41 kya), with probably less harsh winters.

5. Conclusions

The results of this study indicate a variable individual age structure for the different localities studied, mostly differentiated by the fraction of juveniles. The high prevalence of hypoplasia (recorded on about 20 % of the studied teeth) and the mortality curves revealed three general vulnerability periods (birth, weaning, cow-calf separation/maturity) during the lifetime of *C. antiquitatis* individuals that were more or less pronounced depending on the localities. Dietary proxies confirm that *C. antiquitatis* was predominantly grazing in a pure C_3 environment. Several proxies (body mass, dental wear, hypoplasia prevalence) displayed sinusoidal spatio-temporal variations suggesting some flexibility in the dietary preferences (variable grazing), habitat, and physiology of this species in Europe. These variations could be related to climatic changes, whether regional or more global (stadials-interstadials). However, absolute dating of the dental specimens is necessary to precisely correlate the observed variations and specific climatic changes (stadials-interstadials). Stable isotopic analyses revealed mild conditions, consistent with the warmer interval during the OIS3 (59 and 41 kya). The seasonal variations inferred at the studied localities based on isotopic analyses of dental enamel were limited, probably due to the specificity of rhinoceros enamel (not very sensitive to changes in aridity) and isotope damping. Our data on the diet, physiology, and habitat of *C. antiquitatis* highlighted rather strict climatic parameters of the species' niche pointing toward high vulnerability in case of climatic and vegetational changes during the latest Pleistocene.

CRediT authorship contribution statement

Manon Hullot: Writing – review & editing, Writing – original draft, Visualization, Software, Project administration, Methodology, Investigation, Funding acquisition, Conceptualization. **Céline Martin:** Writing – review & editing, Validation, Methodology, Investigation. **Cécile Blondel:** Writing – review & editing, Validation, Methodology. **Damien Becker:** Writing – review & editing, Validation, Conceptualization. **Gertrud E. Rössner:** Writing – review & editing, Validation, Project administration, Funding acquisition, Conceptualization.

Data availability

Raw data are available in the supplementary files.

Declaration of competing interest

The authors declare that they have no known competing financial interests or personal relationships that could have appeared to influence the work reported in this paper.

Acknowledgments

The authors would like to thank the following curators and researchers for granting access and helping in the collections of their institutions: Eli Amson, Thomas Rathgeber, and Achim Lehmkuhl (Staatliches Museum für Naturkunde Stuttgart), João Marreiros, Geoff Carver, and Ivan Calandra (Archäologisches Forchungszentrum und Museum für menschliche Verhaltensevolution Monrepos), Spyridoula Pappa (Natural History Museum of London), Guillaume Billet and Christine Argot (Museum d'Histoire Naturelle de Paris), Natasja den Ouden (Naturalis Leiden), Cécilia Cousin, Julien Lalanne and Annelise Folie (Institute of Natural Sciences, Brussels), Ulrike Stottrop (Museum für Ur-und Ortsgeschichte Bottrop), Emmanuel Robert (Université Lyon 1 Claude Bernard).

This work was funded by a Research Fellowship from the Alexander von Humboldt foundation. Moreover, the SYNTHESYS program covered the expenses for the visits in the collections of the MNHN Paris (FR-TAF_Call4_057) and the RBINS Brussels (BETAF_C4_HULLOT).

Appendix A. Supplementary data

Supplementary data to this article can be found online at https://doi.org/10.1016/j.quaint.2024.10.005.

References

Ackermans, N.L., Martin, L.F., Codron, D., Hummel, J., Kircher, P.R., Richter, H., Kaiser, T.M., Clauss, M., Hatt, J.-M., 2020. Mesowear represents a lifetime signal in sheep (*Ovis aries*) within a long-term feeding experiment. Palaeogeogr. Palaeoclimatol. Palaeoecol. 553, 109793. https://doi.org/10.1016/j.palaeo.2020.109793.

Antoine, P.-O., 2012. Pleistocene and Holocene rhinocerotids (Mammalia, Perissodactyla) from the indochinese peninsula. Comptes Rendus Palevol 11, 159–168. https://doi.org/10.1016/j.crpv.2011.03.002.

Ayliffe, L.K., Lister, A.M., Chivas, A.R., 1992. The preservation of glacial-interglacial climatic signatures in the oxygen isotopes of elephant skeletal phosphate. Palaeogeogr. Palaeoclimatol. Palaeoecol. 99, 179–191. https://doi.org/10.1016/0031-0182(92)90014-V.

Baales, M., 2012. Late middle palaeolithic artefacts and archaeostratigraphical dating of the bone gravels (Knochenkiese) in central Westphalia and the Ruhrgebiet (Germany). In: Niekus, M.L.J., Barton, R.N.E., Street, M., Terberger, Th (Eds.), A Mind Set on Flint: Studies in Honour of Dick Stapert, pp. 119–139. Barkhuis.

Bacon, A.-M., Demeter, F., Tougard, C., Vos, J. de, Sayavongkhamdy, T., Antoine, P.-O., Bouasisengpaseuth, B., Sichanthongtip, P., 2008. Redécouverte d'une faune pléistocène dans les remplissages karstiques de Tam Hang au Laos : Premiers résultats. Comptes Rendus Palevol 7, 277–288. https://doi.org/10.1016/j.crpv.2008.03.009.

Bacon, A.-M., Duringer, P., Antoine, P.-O., Demeter, F., Shackelford, L., Sayavongkhamdy, T., Sichanthongtip, P., Khamdalavong, P., Nokhamaomphu, S., Sysuphanh, V., Patole-Edoumba, E., Chabaux, F., Pelt, E., 2011. The Middle Pleistocene mammalian fauna from Tam Hang karstic deposit, northern Laos: new data and evolutionary hypothesis. Quaternary International, Late Quaternary mammal ecology: insight from new approaches 245, 315–332. https://doi.org/10.1016/j.quaint.2010.11.024.

Bacon, A.-M., Westaway, K., Antoine, P.-O., Duringer, P., Blin, A., Demeter, F., Ponche, J.-L., Zhao, J.-X., Barnes, L.M., Sayavonkhamdy, T., Thuy, N.T.K., Long, V. T., Patole-Edoumba, E., Shackelford, L., 2015. Late Pleistocene mammalian assemblages of Southeast Asia: new dating, mortality profiles and evolution of the predator–prey relationships in an environmental context. Palaeogeogr. Palaeoclimatol. Palaeoecol. 422, 101–127. https://doi.org/10.1016/j.palaeo.2015.01.011.

Bacon, A.-M., Antoine, P.-O., Huong, N.T.M., Westaway, K., Tuan, N.A., Duringer, P., Zhao, J., Ponche, J.-L., Dung, S.C., Nghia, T.H., Minh, T.T., Son, P.T., Boyon, M., Thuy, N.T.K., Blin, A., Demeter, F., 2018. A rhinocerotid-dominated megafauna at the MIS6-5 transition: the late middle Pleistocene Coc Muoi assemblage, lang son province, vietnam. Quat. Sci. Rev. 186, 123–141. https://doi.org/10.1016/j.quascirev.2018.02.017.

Ballatore, M., Merceron, G., Breda, M., 2017. Inferences on the Diet of Fossil European Rhinoceroses: Palaeoecological Inferences from the Dental Material of Pliocene to Early Pleistocene European Rhinoceroses. Lambert Academic Publishing.

Barnosky, A.D., Koch, P.L., Feranec, R.S., Wing, S.L., Shabel, A.B., 2004. Assessing the causes of late Pleistocene extinctions on the continents. Science 306, 70–75. https://doi.org/10.1126/science.1101476.

Bentaleb, I., Langlois, C., Martin, C., Iacumin, P., Carré, M., Antoine, P.-O., Duranthon, F., Moussa, I., Jaeger, J.-J., Barrett, N., 2006. Rhinocerotid tooth enamel $^{18}O/^{16}O$ variability between 23 and 12 Ma in southwestern France. Compt. Rendus Geosci. 338, 172–179. https://doi.org/10.1016/j.crte.2005.11.007.

Berlioz, E., Leduc, C., Hofman-Kamińska, E., Bignon-Lau, O., Kowalczyk, R., Merceron, G., 2022. Dental microwear foraging ecology of a large browsing ruminant in Northern Hemisphere: the European moose (*Alces alces*). Palaeogeogr. Palaeoclimatol. Palaeoecol. 586, 110754. https://doi.org/10.1016/j.palaeo.2021.110754.

Bernard, A., Daux, V., Lécuyer, C., Brugal, J.-P., Genty, D., Wainer, K., Gardien, V., Fourel, F., Jaubert, J., 2009. Pleistocene seasonal temperature variations recorded in the $\delta^{18}O$ of *Bison priscus* teeth. Earth Planet Sci. Lett. 283, 133–143. https://doi.org/10.1016/j.epsl.2009.04.005.

Biasatti, D., Wang, Y., Deng, T., 2018. Paleoecology of Cenozoic rhinos from northwest China: a stable isotope perspective. Vertebr. Palasiat. 56, 45.

Blain, H.-A., Martínez Monzón, A., López-García, J.M., Lozano-Fernández, I., Folie, A., 2019. Amphibians and squamate reptiles from the late Pleistocene of the "Caverne Marie-Jeanne" (Hastière-Lavaux, Namur, Belgium): systematics, paleobiogeography, and paleoclimatic and paleoenvironmental reconstructions. Comptes Rendus Palevol, Palaeobiology and palaeobiogeography of amphibians and reptiles: An homage to Jean-Claude RagePaléobiologie et paléobiogéographie des amphibiens et reptiles : un hommage à Jean-Claude Rage 18, 849–875. https://doi.org/10.1016/j.crpv.2019.04.006.

Boeskorov, G.G., 2012. Some specific morphological and ecological features of the fossil woolly rhinoceros (*Coelodonta antiquitatis* Blumenbach 1799). Biol. Bull. 39, 692–707.

Boeskorov, G.G., Bakulina, N.T., Davydov, S.P., Shchelchkova, M.V., Solomonov, N.G., 2011. Study of pollen and spores from the stomach of a fossil woolly rhinoceros found in the lower reaches of the Kolyma river. In: Doklady Biological Sciences. Springer, pp. 23–25. https://doi.org/10.1134/S0012496611010017.

Boylan, P.J., 2008. The 1858 discovery and excavation of the Brixham bone cave, devon. Stud. Speleol. 16, 3–15.

Brace, S., Palkopoulou, E., Dalén, L., Lister, A.M., Miller, R., Otte, M., Germonpré, M., Blockley, S.P.E., Stewart, J.R., Barnes, I., 2012. Serial population extinctions in a small mammal indicate Late Pleistocene ecosystem instability. Proc. Natl. Acad. Sci. USA 109, 20532–20536. https://doi.org/10.1073/pnas.1213322109.

Bullington, J., 1991. Deciduous dental microwear of prehistoric juveniles from the lower Illinois River Valley. Am. J. Phys. Anthropol. 84, 59–73. https://doi.org/10.1002/ajpa.1330840106.

Carvalho, T.S., Schmid, T.M., Baumann, T., Lussi, A., 2017. Erosive effect of different dietary substances on deciduous and permanent teeth. Clin. Oral Invest. 21, 1519–1526. https://doi.org/10.1007/s00784-016-1915-z.

Çep, B., Schürch, B., Münzel, S.C., Frick, J.A., 2021. Adaptive capacity and flexibility of the Neanderthals at Heidenschmiede (Swabian Jura) with regard to core reduction strategies. PLoS One 16, e0257041.

Cerling, T.E., Harris, J.M., Ambrose, S.H., Leakey, M.G., Solounias, N., 1997. Dietary and environmental reconstruction with stable isotope analyses of herbivore tooth enamel from the Miocene locality of Fort Ternan, Kenya. J. Hum. Evol. 33, 635–650. https://doi.org/10.1006/jhev.1997.0151.

Ciner, B., Wang, Y., Deng, T., Flynn, L., Hou, S., Wu, W., 2015. Stable carbon and oxygen isotopic evidence for Late Cenozoic environmental change in Northern China. Palaeogeogr. Palaeoclimatol. Palaeoecol. 440, 750–762. https://doi.org/10.1016/j.palaeo.2015.10.009.

Clauss, M., Frey, R., Kiefer, B., Lechner-Doll, M., Loehlein, W., Polster, C., Rössner, G.E., Streich, W.J., 2003. The maximum attainable body size of herbivorous mammals: morphophysiological constraints on foregut, and adaptations of hindgut fermenters. Oecologia 136, 14–27. https://doi.org/10.1007/s00442-003-1254-z.

Clauss, M., Polster, C., Kienzle, E., Wiesner, H., Baumgartner, K., Von Houwald, F., Ortmann, S., Streich, W.J., Dierenfeld, E.s., 2005. Studies on digestive physiology and feed digestibilities in captive Indian rhinoceros (*Rhinoceros unicornis*). J. Anim. Physiol. Anim. Nutr. 89, 229–237. https://doi.org/10.1111/j.1439-0396.2005.00546.x.

Comeyne, A., 2013. Taphonomy, osteometry and archaeozoology of the Pleistocene herbivores from the third horizon of the Goyet cave, Belgium. Universiteit, Gent, p. 173. Master Thesis.

Conard, N.J., Bolus, M., 2008. Radiocarbon dating the late middle paleolithic and the aurignacian of the swabian jura. Journal of Human Evolution, Chronology of the Middle-Upper Paleolithic Transition in Eurasia 55, 886–897. https://doi.org/10.1016/j.jhevol.2008.08.006.

Coplen, T.B., Kendall, C., Hopple, J., 1983. Comparison of stable isotope reference samples. Nature 302, 236–238. https://doi.org/10.1038/302236a0.

Damuth, J., 1990. Problems in estimating body masses of archaic ungulates using dental measurements. In: Damuth, J., MacFadden, B.J. (Eds.), Body Size in Mammalian Paleobiology: Estimation and Biological Implications, pp. 229–254. Cambridge.

D'Angela, D., Longinelli, A., 1990. Oxygen isotopes in living mammal's bone phosphate: further results. Chem. Geol. Isot. Geosci. 86, 75–82. https://doi.org/10.1016/0168-9622(90)90007-Y.

Danowitz, M., Hou, S., Mihlbachler, M., Hastings, V., Solounias, N., 2016. A combined-mesowear analysis of late Miocene giraffids from North Chinese and Greek localities of the Pikermian Biome. Palaeogeogr. Palaeoclimatol. Palaeoecol. 449, 194–204. https://doi.org/10.1016/j.palaeo.2016.02.026.

DeSantis, L.R.G., Wallace, S.C., 2008. Neogene forests from the Appalachians of Tennessee, USA: geochemical evidence from fossil mammal teeth. Palaeogeography, Palaeoclimatology, Palaeoecology, Investigating climates, environments and biology using stable isotopes 266, 59–68. https://doi.org/10.1016/j.palaeo.2008.03.032.

Diedrich, C.G., 2012. Late Pleistocene *Crocuta crocuta spelaea* (Goldfuss 1823) populations from the Emscher River terrace open air hyena den near Bottrop and other sites in NW Germany: their bone accumulations along rivers in lowland mammoth steppe environments and scavenging activities on woolly rhinoceros. In: Quaternary International, Mammoths and Their Relatives 2: Biotopes, Evolution and Human Impact V International Conference, Le Puy-En-Velay, vol. 2010, pp. 93–119. https://doi.org/10.1016/j.quaint.2011.07.046, 276–277.

Dinerstein, E., 2011. Family Rhinocerotidae (rhinoceroses). In: Wilson, D.E., Mittemeier, R.A. (Eds.), Handbook of the Mammals of the World. Lynx Edicions, Barcelona, pp. 144–181.

Dobney, K., Ervynck, A., 2000. Interpreting developmental stress in archaeological pigs: the chronology of linear enamel hypoplasia. J. Archaeol. Sci. 27, 597–607. https://doi.org/10.1006/jasc.1999.0477.

Domingo, L., Koch, P.L., Fernández, M.H., Fox, D.L., Domingo, M.S., Alberdi, M.T., 2013. Late neogene and early quaternary paleoenvironmental and paleoclimatic conditions in southwestern Europe: isotopic analyses on mammalian taxa. PLoS One 8, e63739. https://doi.org/10.1371/journal.pone.0063739.

Ensor, B.E., Irish, J.D., 1995. Hypoplastic area method for analyzing dental enamel hypoplasia. Am. J. Phys. Anthropol. 98, 507–517. https://doi.org/10.1002/ajpa.1330980410.

Fernandez, P., Legendre, S., 2003. Mortality curves for horses from the Middle Palaeolithic site of Bau de l'Aubesier (Vaucluse, France): methodological, palaeo-ethnological, and palaeo-ecological approaches. J. Archaeol. Sci. 30, 1577–1598. https://doi.org/10.1016/S0305-4403(03)00054-2.

Ferring, R., Oms, O., Agustí, J., Berna, F., Nioradze, M., Shelia, T., Tappen, M., Vekua, A., Zhvania, D., Lordkipanidze, D., 2011. Earliest Human Occupations at Dmanisi (Georgian Caucasus) Dated to 1.85–1.78 Ma, vol. 108. Proceedings of the National Academy of Sciences, pp. 10432–10436.

Fortelius, M., 1982. Ecological aspects of dental functional morphology in the Plio-Pleistocene rhinoceroses of Europe. In: Teeth: Form, Function, and Evolution. Columbia University Press, pp. 163–181.

Fortelius, M., Kappelman, J., 1993. The largest land mammal ever imagined. Zool. J. Linn. Soc. 108, 85–101. https://doi.org/10.1006/zjls.1993.1018.

Fortelius, M., Solounias, N., 2000. Functional characterization of ungulate molars using the abrasion-attrition wear gradient: a new method for reconstructing paleodiets. Am. Mus. Novit. 2000, 1–36.

Fourvel, J.-B., Fosse, P., Fernandez, P., Antoine, P.-O., 2015. Large mammals of Fouvent-Saint-Andoche (Haute-Saône, France): a glimpse into a late Pleistocene hyena den. Geodiversitas 37, 237–266. https://doi.org/10.5252/g2015n2a5.

Francisco, A., Blondel, C., Brunetière, N., Ramdarshan, A., Merceron, G., 2018. Enamel surface topography analysis for diet discrimination. A methodology to enhance and select discriminative parameters. Surface Topography: Metrology and Properties 6, 015002. https://doi.org/10.1088/2051-672X/aa9dd3.

Franz-Odendaal, T.A., Lee-Thorp, J.A., Chinsamy, A., 2003. Insights from stable light isotopes on enamel defects and weaning in Pliocene herbivores. J. Biosci. 28, 765–773. https://doi.org/10.1007/BF02708437.

Garutt, N.V., 1994. Dental ontogeny of the woolly rhinoceros *Coelodonta antiquitatis* (Blumenbach, 1799). CRANIUM 11, 37–48.

Geel van, B., Langeveld, B.W., Mol, D., Knaap van der, P.W.O, Leeuwen van, J.F.N., 2019. Pollen and spores from molar folds reflect food choice of late Pleistocene and Early Holocene herbivores in The Netherlands and the adjacent North Sea area. Quat. Sci. Rev. 225, 106030. https://doi.org/10.1016/j.quascirev.2019.106030.

Genty, D., Combourieu-Nebout, N., Peyron, O., Blamart, D., Wainer, K., Mansuri, F., Ghaleb, B., Isabello, L., Dormoy, I., Grafenstein, U. von, Bonelli, S., Landais, A., Brauer, A., 2010. Isotopic characterization of rapid climatic events during OIS3 and OIS4 in Villars Cave stalagmites (SW-France) and correlation with Atlantic and Mediterranean pollen records. Quaternary Science Reviews, Special Theme: Case Studies of Neodymium Isotopes in Paleoceanography 29, 2799–2820. https://doi.org/10.1016/j.quascirev.2010.06.035.

Germonpré, M., 1993. Taphonomy of Pleistocene mammal assemblages of the flemish valley, Belgium. Bulletin de l'Institut royal des Sciences naturelles de Belgique, Sciences de la Terre 63, 271–309.
Germonpré, M., Sablin, M.V., 2001. The cave bear (*Ursus spelaeus*) from Goyet, Belgium. The bear den in Chamber B (bone horizon 4). Bulletin de l'Institut Royal des Sciences de Belgiques. Science de la Terre 71, 209–233.
Gibbard, P.L., Head, M.J., 2020. Chapter 30 - The Quaternary period. In: Gradstein, F.M., Ogg, J.G., Schmitz, M.D., Ogg, G.M. (Eds.), Geologic Time Scale 2020. Elsevier, pp. 1217–1255. https://doi.org/10.1016/B978-0-12-824360-2.00030-9.
Goddard, J., 1970. Food preferences of black rhinoceros in the Tsavo national Park. East Afr. Wildl. J. 8, 145–161. https://doi.org/10.1111/j.1365-2028.1970.tb00837.x.
Goodman, A.H., Rose, J.C., 1990. Assessment of systemic physiological perturbations from dental enamel hypoplasias and associated histological structures. Am. J. Phys. Anthropol. 33, 59–110. https://doi.org/10.1002/ajpa.1330330506.
Goodman, A.H., Rose, J.C., 1991. Dental enamel hypoplasias as indicators of nutritional status. In: Kelley, M., Larsen, C. (Eds.), Advances in Dental Anthropology, pp. 279–293.
Gordon, K.D., 1982. A study of microwear on chimpanzee molars: implications for dental microwear analysis. Am. J. Phys. Anthropol. 59, 195–215. https://doi.org/10.1002/ajpa.1330590208.
Guatelli-Steinberg, D., 2001. What can developmental defects of enamel reveal about physiological stress in nonhuman primates? Evol. Anthropol. 10, 138–151. https://doi.org/10.1002/evan.1027.
Guérin, C., 1980. Les rhinocéros (Mammalia, Perissodactyla) du Miocène terminal au Pleistocène supérieur en Europe occidentale: comparaison avec les espèces actuelles. Documents de l'Université de Lyon, Villeurbanne.
Guérin, C., Philippe, M., Vilain, R., 1979. Le gisement pléistocène supérieur de Jaurens à Nespouls, Corrèze, France : Historique et généralités, vol. 17. Publications du musée des Confluences, pp. 11–16. https://doi.org/10.3406/mhnly.1979.1039.
Hamilton, I.M., Barclay, R.M.R., 1998. Diets of juvenile, yearling, and adult big Brown bats (*Eptesicus fuscus*) in southeastern alberta. J. Mammal. 79, 764–771. https://doi.org/10.2307/1383087.
Hamilton, N.E., Ferry, M., 2018. Ggtern: ternary diagrams using ggplot2. J. Stat. Software 87, 1–17. https://doi.org/10.18637/jss.v087.c03.
Harris, E.B., Kohn, M.J., Strömberg, C.A.E., 2020. Stable isotope compositions of herbivore teeth indicate climatic stability leading into the mid-Miocene Climatic Optimum, in Idaho, U.S.A. Palaeogeogr. Palaeoclimatol. Palaeoecol. 546, 109610. https://doi.org/10.1016/j.palaeo.2020.109610.
Hedges, R.E.M., Pettitt, P.B., Ramsey, C.B., Klinken, G.J.V., 1996. Radiocarbon dates from the oxford ams system: archaeometry DATELIST 22. Archaeometry 38, 391–415. https://doi.org/10.1111/j.1475-4754.1996.tb00785.x.
Hernesniemi, E., Blomstedt, K., Fortelius, M., 2011. Multi-view stereo three-dimensional reconstruction of lower molars of recent and Pleistocene rhinoceroses for mesowear analysis. Palaeontol. Electron. 14, 1–15.
Hillman-Smith, A.K.K., Owen-Smith, N.R., Anderson, J.L., Hall-Martin, A.J., Selaladi, J. P., 1986. Age estimation of the white rhinoceros (*Ceratotherium simum*). J. Zool. 210, 355–377.
Hitchins, P.M., 1978. Age determination of the black rhinoceros (*Diceros bicornis* Linn.) in Zululand. S. Afr. J. Wildl. Res. 8, 71–80.
Hopkins, S.S.B., 2018. Estimation of Body Size in Fossil Mammals. In: Croft, D.A., Su, D. F., Simpson, S.W. (Eds.), Methods in Paleoecology: Reconstructing Cenozoic Terrestrial Environments and Ecological Communities, Vertebrate Paleobiology and Paleoanthropology. Springer International Publishing, Cham, pp. 7–22. https://doi.org/10.1007/978-3-319-94265-0_2.
Hullot, M., Antoine, P.-O., 2020. Mortality curves and population structures of late early Miocene Rhinocerotidae (Mammalia, Perissodactyla) remains from the Béon 1 locality of Montréal-du-Gers, France. Palaeogeogr. Palaeoclimatol. Palaeoecol. 558, 109938. https://doi.org/10.1016/j.palaeo.2020.109938.
Hullot, M., Antoine, P.-O., 2022. Enamel hypoplasia on rhinocerotoid teeth: Does CT-scan imaging detect the defects better than the naked eye? Palaeovertebrata 45, e2. https://doi.org/10.18563/pv.45.1.e2.
Hullot, M., Antoine, P.-O., Ballatore, M., Merceron, G., 2019. Dental microwear textures and dietary preferences of extant rhinoceroses (Perissodactyla, Mammalia). Mammal Research 64, 397–409. https://doi.org/10.1007/s13364-019-00427-4.
Hullot, M., Laurent, Y., Merceron, G., Antoine, P.-O., 2021. Paleoecology of the Rhinocerotidae (Mammalia, Perissodactyla) from Béon 1, Montréal-du-Gers (late early Miocene, SW France): Insights from dental microwear texture analysis, mesowear, and enamel hypoplasia. Palaeontol. Electron. 24, 1–26. https://doi.org/10.26879/1163.
Hullot, M., Merceron, G., Antoine, P.-O., 2023. Spatio-temporal diversity of dietary preferences and stress sensibilities of early and middle Miocene Rhinocerotidae from Eurasia: impact of climate changes. Peer Community Journal 3. https://doi.org/10.24072/pcjournal.222 article e5.
Janis, C.M., 1988. An Estimation of Tooth Volume and Hypsodonty Indices in Ungulate Mammals, and the Correlation of These Factors with Dietary Preferences, vol. 53. Memoires du Museum National d' Histoire Naturelle serie C, pp. 367–387.
Janis, C.M., 1990. Correlation of cranial and dental variables with body size in ungulates and macropodoids. In: Damuth, J., MacFadden, B.J. (Eds.), Body Size in Mammalian Paleobiology: Estimation and Biological Implications. Cambridge University Press, Cambridge, pp. 255–300.
Jansen, F., Drozdzewski, G., 1986. Erläuterungen zu Blatt 4507 Mülheim an der Ruhr. Erläuterungen zur Geologischen Karte von Nordrhein-Westfalen, 1e200. Krefeld.
Jarek, S., 2012. mvnormtest: Normality test for multivariate variables. R package version 0, 1–9.
Jeglinski, J.W.E., Goetz, K.T., Werner, C., Costa, D.P., Trillmich, F., 2013. Same size – same niche? Foraging niche separation between sympatric juvenile Galapagos sea lions and adult Galapagos fur seals. J. Anim. Ecol. 82, 694–706. https://doi.org/10.1111/1365-2656.12019.
Kelly, A., Miller, J.H., Wooller, M.J., Seaton, C.T., Druckenmiller, P., DeSantis, L., 2021. Dietary paleoecology of bison and horses on the mammoth steppe of eastern Beringia based on dental microwear and mesowear analyses. Palaeogeogr. Palaeoclimatol. Palaeoecol. 572, 110394. https://doi.org/10.1016/j.palaeo.2021.110394.
Koch, P.L., Barnosky, A.D., 2006. Late Quaternary Extinctions: State of the Debate. Annual Review of Ecology. Evolution, and Systematics 37, 215–250. https://doi.org/10.1146/annurev.ecolsys.34.011802.132415.
Koenigswald, W. von, Müller-Beck, H., 1975. Das Pleistozän der Weinberghöhlen bei Mauern (Bayern)(Nachtrag 1975). Quartär–Internationales Jahrbuch zur Erforschung des Eiszeitalters und der Steinzeit 26, 107–118.
Kosintsev, P., Mitchell, K.J., Devièse, T., Plicht van der, J., Kuitems, M., Petrova, E., Tikhonov, A., Higham, T., Comeskey, D., Turney, C., 2019. Evolution and extinction of the giant rhinoceros *Elasmotherium sibiricum* sheds light on late Quaternary megafaunal extinctions. Nature ecology & evolution 3, 31. https://doi.org/10.1038/s41559-018-0722-0.
Kühl, N., Litt, T., Schölzel, C., Hense, A., 2007. Eemian and Early Weichselian temperature and precipitation variability in northern Germany. Quat. Sci. Rev. 26, 3311–3317. https://doi.org/10.1016/j.quascirev.2007.10.004.
Kuzmin, Y.V., 2010. Extinction of the woolly mammoth (*Mammuthus primigenius*) and woolly rhinoceros (*Coelodonta antiquitatis*) in Eurasia: review of chronological and environmental issues. Boreas 39, 247–261.
Laurie, W.A., Lang, E.M., Groves, C.P., 1983. *Rhinoceros unicornis*. Mamm. Species 211, 1–6. https://doi.org/10.2307/3504002.
Lécuyer, C., Balter, V., Martineau, F., Fourel, F., Bernard, A., Amiot, R., Gardien, V., Otero, O., Legendre, S., Panczer, G., Simon, L., Martini, R., 2010. Oxygen isotope fractionation between apatite-bound carbonate and water determined from controlled experiments with synthetic apatites precipitated at 10–37°C. Geochem. Cosmochim. Acta 74, 2072–2081. https://doi.org/10.1016/j.gca.2009.12.024.
Legendre, S., 1989. Les communautés de mammifères du Paléogène (Eocène supérieur et Oligocène) d'Europe occidentale : Structures, milieux et évolution. Münchner Geowissenschaftliche Abhandlungen, München, Germany.
Levin, N.E., Cerling, T.E., Passey, B.H., Harris, J.M., Ehleringer, J.R., 2006. A stable isotope aridity index for terrestrial environments. Proc. Natl. Acad. Sci. USA 103, 11201–11205. https://doi.org/10.1073/pnas.0604719103.
Lisiecki, L.E., Raymo, M.E., 2005. A Pliocene-Pleistocene stack of 57 globally distributed benthic $\delta^{18}O$ records. Paleoceanography 20. https://doi.org/10.1029/2004PA001071.
López-García, J.M., Blain, H.-A., Lozano-Fernández, I., Luzi, E., Folie, A., 2017. Environmental and climatic reconstruction of MIS 3 in northwestern Europe using the small-mammal assemblage from Caverne Marie-Jeanne (Hastière-Lavaux, Belgium). Palaeogeogr. Palaeoclimatol. Palaeoecol. 485, 622–631. https://doi.org/10.1016/j.palaeo.2017.07.017.
Lord, E., Dussex, N., Kierczak, M., Díez-del-Molino, D., Ryder, O.A., Stanton, D.W.G., Gilbert, M.T.P., Sánchez-Barreiro, F., Zhang, G., Sinding, M.-H.S., Lorenzen, E.D., Willerslev, E., Protopopov, A., Shidlovskiy, F., Fedorov, S., Bocherens, H., Nathan, S. K.S.S., Goossens, B., Plicht van der, J., Chan, Y.L., Prost, S., Potapova, O., Kirillova, I., Lister, A.M., Heintzman, P.D., Kapp, J.D., Shapiro, B., Vartanyan, S., Götherström, A., Dalén, L., 2020. Pre-extinction Demographic Stability and Genomic Signatures of Adaptation in the Woolly Rhinoceros. Curr. Biol. 30, 3871–3879.e7. https://doi.org/10.1016/j.cub.2020.07.046.
Lorenzen, E.D., Nogués-Bravo, D., Orlando, L., Weinstock, J., Binladen, J., Marske, K.A., Ugan, A., Borregaard, M.K., Gilbert, M.T.P., Nielsen, R., Ho, S.Y.W., Goebel, T., Graf, K.E., Byers, D., Stenderup, J.T., Rasmussen, M., Campos, P.F., Leonard, J.A., Koepfli, K.-P., Froese, D., Zazula, G., Stafford, T.W., Aaris-Sørensen, K., Batra, P., Haywood, A.M., Singarayer, J.S., Valdes, P.J., Boeskorov, G., Burns, J.A., Davydov, S.P., Haile, J., Jenkins, D.L., Kosintsev, P., Kuznetsova, T., Lai, X., Martin, L.D., McDonald, H.G., Mol, D., Meldgaard, M., Munch, K., Stephan, E., Sablin, M., Sommer, R.S., Sipko, T., Scott, E., Suchard, M.A., Tikhonov, A., Willerslev, R., Wayne, R.K., Cooper, A., Hofreiter, M., Sher, A., Shapiro, B., Rahbek, C., Willerslev, E., 2011. Species-specific responses of Late Quaternary megafauna to climate and humans. Nature 479, 359–364. https://doi.org/10.1038/nature10574.
MacFadden, B.J., Higgins, P., 2004. Ancient ecology of 15-million-year-old browsing mammals within C3 plant communities from Panama. Oecologia 140, 169–182. https://doi.org/10.1007/s00442-004-1571-x.
Martin, C., Bentaleb, I., Kaandorp, R., Iacumin, P., Chatri, K., 2008. Intra-tooth study of modern rhinoceros enamel $\delta^{18}O$: Is the difference between phosphate and carbonate $\delta^{18}O$ a sound diagenetic test? Palaeogeography, Palaeoclimatology, Palaeoecology, Beyond documenting diagenesis: The fifth international bone diagenesis workshop 266, 183–189. https://doi.org/10.1016/j.palaeo.2008.03.039.
Mead, A.J., 1999. Enamel hypoplasia in Miocene rhinoceroses (*Teleoceras*) from Nebraska: evidence of severe physiological stress. J. Vertebr. Paleontol. 19, 391–397. https://doi.org/10.1080/02724634.1999.10011150.
Metcalfe, J.Z., Longstaffe, F.J., Zazula, G.D., 2010. Nursing, weaning, and tooth development in woolly mammoths from Old Crow, Yukon, Canada: Implications for Pleistocene extinctions. Palaeogeogr. Palaeoclimatol. Palaeoecol. 298, 257–270. https://doi.org/10.1016/j.palaeo.2010.09.032.
Mihlbachler, M.C., 2003. Demography of late Miocene rhinoceroses (*Teleoceras proterum* and *Aphelops malacorhinus*) from Florida: linking mortality and sociality in fossil assemblages. Paleobiology 29, 412–428. https://doi.org/10.1666/0094-8373(2003)029<0412:DOLMRT>2.0.CO;2.
Mihlbachler, M.C., Rivals, F., Solounias, N., Semprebon, G.M., 2011. Dietary change and evolution of horses in North America. Science 331, 1178–1181. https://doi.org/10.1126/science.1196166.

Mihlbachler, M.C., Campbell, D., Chen, C., Ayoub, M., Kaur, P., 2018. Microwear–mesowear congruence and mortality bias in rhinoceros mass-death assemblages. Paleobiology 44, 131–154. https://doi.org/10.1017/pab.2017.13.
Mogensen, I.A., 2009. Dansgaard-Oeschger Cycles. In: Gornitz, V. (Ed.), Encyclopedia of Paleoclimatology and Ancient Environments. Springer, Netherlands, Dordrecht, pp. 229–233. https://doi.org/10.1007/978-1-4020-4411-3_55.
Mol, D., Post, K., Reumer, J.W.F., Plicht van der, J., Vos, J. de, Geel van, B., Reenen van, G., Pals, J.P., Glimmerveen, J., 2006. The Eurogeul—first report of the palaeontological, palynological and archaeological investigations of this part of the North Sea. Quaternary International, Third International Mammoth Conference, Dawson, Yukon 142–143, 178–185. https://doi.org/10.1016/j.quaint.2005.03.015.
Mundy, P.J., 1984. Rhinoceros in South and South West Africa. Presented at the Proceedings of a Workshop Held at Pilanesberg Game Reserve, Bophuthatswana.
Niven, L.B., Egeland, C.P., Todd, L.C., 2004. An inter-site comparison of enamel hypoplasia in bison: implications for paleoecology and modeling Late Plains Archaic subsistence. J. Archaeol. Sci. 31, 1783–1794. https://doi.org/10.1016/j.jas.2004.06.001.
Orlandi-Oliveras, G., Köhler, M., Clavel, J., Scott, R.S., Mayda, S., Merceron, G., 2022. Feeding strategies of circum-Mediterranean hipparionins during the late Miocene: Exploring dietary preferences related to size through dental microwear analysis. Palaeontol. Electron. 25, 1–45. https://doi.org/10.26879/990.
Owen-Smith, N.R., 1988. Megaherbivores: the Influence of Very Large Body Size on Ecology. Cambridge University Press, Cambridge.
Pandolfi, L., Boscato, P., Crezzini, J., Gatta, M., Moroni, A., Rolfo, M., Tagliacozzo, A., 2017. Late Pleistocene last occurences of the narrow-nosed rhinoceros *Stephanorhinus hemitoechus* (Mammalia, Perissodactyla) in Italy. Riv. Ital. Paleontol. Stratigr. 123, 177–192. https://doi.org/10.13130/2039-4942/8300.
Peters, R.H., 1983. The Ecological Implications of Body Size. Cambridge University Press, Cambridge.
Pienaar, D., 1994. Social organization and behaviour of the white rhinoceros. In: Proceedings of a Symposium on "Rhinos as Game Ranch Animals." Onderstepoort, Reoublic of South Africa, pp. 87–92.
Polis, G.A., 1984. Age Structure Component of Niche Width and Intraspecific Resource Partitioning: Can Age Groups Function as Ecological Species? Am. Nat. 123, 541–564. https://doi.org/10.1086/284221.
Pushkina, D., Bocherens, H., Ziegler, R., 2014. Unexpected palaeoecological features of the Middle and Late Pleistocene large herbivores in southwestern Germany revealed by stable isotopic abundances in tooth enamel. Quaternary International, Fossil remains. karst and their role in reconstructing Quaternary paleoclimate and paleoenvironments 164–178. https://doi.org/10.1016/j.quaint.2013.12.033, 339–340.
Rey, K., Amiot, R., Lécuyer, C., Koufos, G.D., Martineau, F., Fourel, F., Kostopoulos, D.S., Merceron, G., 2013. Late Miocene climatic and environmental variations in northern Greece inferred from stable isotope compositions ($\delta^{18}O$, $\delta^{13}C$) of equid teeth apatite. Palaeogeogr. Palaeoclimatol. Palaeoecol. 388, 48–57. https://doi.org/10.1016/j.palaeo.2013.07.021.
Rey-Iglesia, A., Lister, A.M., Stuart, A.J., Bocherens, H., Szpak, P., Willerslev, E., Lorenzen, E.D., 2021. Late Pleistocene paleoecology and phylogeography of woolly rhinoceroses. Quat. Sci. Rev. 263, 106993. https://doi.org/10.1016/j.quascirev.2021.106993.
Ripley, B., Venables, B., Bates, D.M., Hornik, K., Gebhardt, A., Firth, D., Ripley, M.B., 2013. Package 'mass, vol. 538. ' Cran r, pp. 113–120.
Rivals, F., Lister, A.M., 2016. Dietary flexibility and niche partitioning of large herbivores through the Pleistocene of Britain. Quat. Sci. Rev. 146, 116–133. https://doi.org/10.1016/j.quascirev.2016.06.007.
Saarinen, J., Eronen, J., Fortelius, M., Seppä, H., Lister, A.M., 2016. Patterns of diet and body mass of large ungulates from the Pleistocene of Western Europe, and their relation to vegetation. Palaeontol. Electron. 19, 1–58. https://doi.org/10.26879/443.
Saarinen, J., Mantzouka, D., Sakala, J., 2020. Aridity, Cooling, Open Vegetation, and the Evolution of Plants and Animals During the Cenozoic. In: Martinetto, E., Tschopp, E., Gastaldo, R.A. (Eds.), Nature through Time, Springer Textbooks in Earth Sciences, Geography and Environment. Springer International Publishing, Cham, pp. 83–107. https://doi.org/10.1007/978-3-030-35058-1_3.
Sánchez Chillón, B., Alberdi, M.T., Leone, G., Bonadonna, F.P., Stenni, B., Longinelli, A., 1994. Oxygen isotopic composition of fossil equid tooth and bone phosphate: an archive of difficult interpretation. Palaeogeography, Palaeoclimatology, Palaeoecology, Stable Isotope and Trace-Element Geochemistry of Vertebrate Fossils: Interpreting Ancient Diets and Climates 107, 317–328. https://doi.org/10.1016/0031-0182(94)90103-1.
Schultz, J.A., Engels, S., Schwermann, L.C., Koenigswald, W. v, 2020. Evolutionary trends in the mastication patterns in some perissodactyls, cetartiodactyls, and proboscideans. In: Mammalian Teeth – Form and Function. Verlag Dr. Friedrich Pfeil, München, Germany, pp. 215–230.
Scott, R.S., Ungar, P.S., Bergstrom, T.S., Brown, C.A., Grine, F.E., Teaford, M.F., Walker, A., 2005. Dental microwear texture analysis shows within-species diet variability in fossil hominins. Nature 436, 693–695. https://doi.org/10.1038/nature03822.
Scott, R.S., Ungar, P.S., Bergstrom, T.S., Brown, C.A., Childs, B.E., Teaford, M.F., Walker, A., 2006. Dental microwear texture analysis: technical considerations. J. Hum. Evol. 51, 339–349. https://doi.org/10.1016/j.jhevol.2006.04.006.
Shao, Y., Limberg, H., Klein, K., Wegener, C., Schmidt, I., Weniger, G.-C., Hense, A., Rostami, M., 2021. Human-existence probability of the Aurignacian techno-complex under extreme climate conditions. Quat. Sci. Rev. 263, 106995. https://doi.org/10.1016/j.quascirev.2021.106995.
Skinner, M.F., Pruetz, J.D., 2012. Reconstruction of periodicity of repetitive linear enamel hypoplasia from perikymata counts on imbricational enamel among dry-adapted chimpanzees (*Pan troglodytes verus*) from Fongoli, Senegal. Am. J. Phys. Anthropol. 149, 468–482. https://doi.org/10.1002/ajpa.22145.
Skinner, M.F., Skinner, M.M., 2017. Orangutans, enamel defects, and developmental health: A comparison of Borneo and Sumatra. Am. J. Primatol. 79, e22668. https://doi.org/10.1002/ajp.22668.
Skrzypek, G., Wiśniewski, A., Grierson, P.F., 2011. How cold was it for Neanderthals moving to Central Europe during warm phases of the last glaciation? Quat. Sci. Rev. 30, 481–487. https://doi.org/10.1016/j.quascirev.2010.12.018.
Stefaniak, K., Stachowicz-Rybka, R., Borówka, R.K., Hrynowiecka, A., Sobczyk, A., Hoyo, M.M., Kotowski, A., Nowakowski, D., Krajcarz, M.T., Billia, E.M.E., Persico, D., Burkanova, E.M., Leschinskiy, S.V., Asperen van, E., Ratajczak, U., Shpansky, A.V., Lempart, M., Wach, B., Niska, M., Made van der, J., Stachowicz, K., Lenarczyk, J., Piątek, J., Kovalchuk, O., 2020. Browsers, grazers or mix-feeders? Study of the diet of extinct Pleistocene Eurasian forest rhinoceros *Stephanorhinus kirchbergensis* (Jäger, 1839) and woolly rhinoceros *Coelodonta antiquitatis* (Blumenbach, 1799). Quat. Int. 605–606, 192–212. https://doi.org/10.1016/j.quaint.2020.08.039.
Steuer, P., Südekum, K.-H., Tütken, T., Müller, D.W.H., Kaandorp, J., Bucher, M., Clauss, M., Hummel, J., 2014. Does body mass convey a digestive advantage for large herbivores? Funct. Ecol. 28, 1127–1134. https://doi.org/10.1111/1365-2435.12275.
Stevens, R.E., O'Connell, T.C., Hedges, R.E.M., Street, M., 2009. Radiocarbon and stable isotope investigations at the Central Rhineland sites of Gönnersdorf and Andernach-Martinsberg, Germany. J. Hum. Evol. 57, 131–148. https://doi.org/10.1016/j.jhevol.2009.01.011.
Street, M., Terberger, T., 2004. The Radiocarbon Chronology of the German Upper Palaeolithic: Fifteen Years of Cooperation with ORAU, vol. 62. OXFORD UNIVERSITY SCHOOL OF ARCHAEOLOGY MONOGRAPH, p. 281.
Strömberg, C.A., 2011. Evolution of grasses and grassland ecosystems. Annu. Rev. Earth Planet Sci. 39, 517–544. https://doi.org/10.1146/annurev-earth-040809-152402.
Stuart, A.J., 1991. Mammalian Extinctions in the Late Pleistocene of Northern Eurasia and North America. Biol. Rev. 66, 453–562. https://doi.org/10.1111/j.1469-185X.1991.tb01149.x.
Stuart, A.J., Lister, A.M., 2007. Patterns of Late Quaternary megafaunal extinctions in Europe and northern Asia. Cour. Forschungsinst. Senckenberg 259, 287.
Stuart, A.J., Lister, A.M., 2012. Extinction chronology of the woolly rhinoceros *Coelodonta antiquitatis* in the context of late Quaternary megafaunal extinctions in northern Eurasia. Quat. Sci. Rev. 51, 1–17. https://doi.org/10.1016/j.quascirev.2012.06.007.
Taylor, L.A., Kaiser, T.M., Schwitzer, C., Müller, D.W.H., Codron, D., Clauss, M., Schulz, E., 2013. Detecting Inter-Cusp and Inter-Tooth Wear Patterns in Rhinocerotids. PLoS One 8, e80921. https://doi.org/10.1371/journal.pone.0080921.
Teaford, M.F., Oyen, O.J., 1989. In vivo and in vitro turnover in dental microwear. Am. J. Phys. Anthropol. 80, 447–460. https://doi.org/10.1002/ajpa.1330800405.
Teaford, M.F., Walker, A., 1984. Quantitative differences in dental microwear between primate species with different diets and a comment on the presumed diet of *Sivapithecus*. Am. J. Phys. Anthropol. 64, 191–200. https://doi.org/10.1002/ajpa.1330640213.
Tejada-Lara, J.V., MacFadden, B.J., Bermudez, L., Rojas, G., Salas-Gismondi, R., Flynn, J. J., 2018. Body mass predicts isotope enrichment in herbivorous mammals. Proc. Biol. Sci. 285, 20181020. https://doi.org/10.1098/rspb.2018.1020.
Tipple, B.J., Meyers, S.R., Pagani, M., 2010. Carbon isotope ratio of Cenozoic CO2: A comparative evaluation of available geochemical proxies. Paleoceanogr. Paleoclimatol. 25. https://doi.org/10.1029/2009PA001851.
Turvey, S.T., Sathe, V., Crees, J.J., Jukar, A.M., Chakraborty, P., Lister, A.M., 2021. Late Quaternary megafaunal extinctions in India: How much do we know? Quat. Sci. Rev. 252, 106740. https://doi.org/10.1016/j.quascirev.2020.106740.
Tütken, T., Vennemann, T.W., Janz, H., Heizmann, E.P.J., 2006. Palaeoenvironment and palaeoclimate of the Middle Miocene lake in the Steinheim basin, SW Germany: A reconstruction from C, O, and Sr isotopes of fossil remains. Palaeogeogr. Palaeoclimatol. Palaeoecol. 241, 457–491. https://doi.org/10.1016/j.palaeo.2006.04.007.
Upex, B., Dobney, K., 2012. Dental enamel hypoplasia as indicators of seasonal environmental and physiological impacts in modern sheep populations: a model for interpreting the zooarchaeological record. J. Zool. 287, 259–268. https://doi.org/10.1111/j.1469-7998.2012.00912.x.
Uzunidis, A., Rivals, F., 2023. Where and when? Combining dental wear and death seasons to improve paleoenvironmental reconstruction through ungulate diets. J. Archaeol. Sci.: Reports 52, 104258. https://doi.org/10.1016/j.jasrep.2023.104258.
Uzunidis, A., Antoine, P.-O., Brugal, J.-P., 2022. A Middle Pleistocene *Coelodonta antiquitatis praecursor* Guérin (1980) (Mammalia, Perissodactyla) from Les Rameaux, SW France, and a revised phylogeny of *Coelodonta* Bronn, 1831. Quat. Sci. Rev. 288, 107594. https://doi.org/10.1016/j.quascirev.2022.107594.
Vandenberghe, J., Pissart, A., 1993. Permafrost changes in Europe during the last glacial. Permafr. Periglac. Process. 4, 121–135. https://doi.org/10.1002/ppp.3430040205.
Wasserstein, R.L., Lazar, N.A., 2016. The ASA Statement on p-Values: Context, Process, and Purpose. Am. Statistician 70, 129–133. https://doi.org/10.1080/00031305.2016.1154108.
Wickham, H., 2016. ggplot2: Elegant Graphics for Data Analysis. Springer-Verlag, New York.
Wickham, H., Henry, L., 2020. Tidyr: Tidy messy data. R package version 1, 397.

Wilke, C.O.. cowplot: Streamlined Plot Theme and Plot Annotations for "ggplot2". R package version 1.1.0. https://CRAN.R-project.org/package=cowplot.

Willerslev, E., Davison, J., Moora, M., Zobel, M., Coissac, E., Edwards, M.E., Lorenzen, E. D., Vestergård, M., Gussarova, G., Haile, J., Craine, J., Gielly, L., Boessenkool, S., Epp, L.S., Pearman, P.B., Cheddadi, R., Murray, D., Bråthen, K.A., Yoccoz, N., Binney, H., Cruaud, C., Wincker, P., Goslar, T., Alsos, I.G., Bellemain, E., Brysting, A. K., Elven, R., Sønstebø, J.H., Murton, J., Sher, A., Rasmussen, M., Rønn, R., Mourier, T., Cooper, A., Austin, J., Möller, P., Froese, D., Zazula, G., Pompanon, F., Rioux, D., Niderkorn, V., Tikhonov, A., Savvinov, G., Roberts, R.G., MacPhee, R.D.E., Gilbert, M.T.P., Kjær, K.H., Orlando, L., Brochmann, C., Taberlet, P., 2014. Fifty thousand years of Arctic vegetation and megafaunal diet. Nature 506, 47–51. https://doi.org/10.1038/nature12921.

Wohlfarth, B., 2013. A review of Early Weichselian climate (MIS 5d-a) in Europe. In: Technical report/Svensk Kärnbränslehantering AB 44.

Xafis, A., Saarinen, J., Bastl, K., Nagel, D., Grímsson, F., 2020. Palaeodietary traits of large mammals from the middle Miocene of Gračanica (Bugojno Basin, Bosnia-Herzegovina). Palaeobiodivers. Palaeoenviron. 100, 457–477. https://doi.org/10.1007/s12549-020-00435-2.

Yurtsev, B.A., 2001. The Pleistocene "Tundra-Steppe" and the productivity paradox: the landscape approach. Quaternary Science Reviews, Beringian Paleoenvironments - Festschrift in Honour of D.M. Hopkins 20, 165–174. https://doi.org/10.1016/S0277-3791(00)00125-6.

Zachos, J.C., Shackleton, N.J., Revenaugh, J.S., Pälike, H., Flower, B.P., 2001. Climate Response to Orbital Forcing Across the Oligocene-Miocene Boundary. Science 292, 274–278. https://doi.org/10.1126/science.1058288.

Zanazzi, A., Kohn, M.J., 2008. Ecology and physiology of White River mammals based on stable isotope ratios of teeth. Palaeogeogr. Palaeoclimatol. Palaeoecol. 257, 22–37. https://doi.org/10.1016/j.palaeo.2007.08.007.

Zanazzi, A., Judd, E., Fletcher, A., Bryant, H., Kohn, M.J., 2015. Eocene–Oligocene latitudinal climate gradients in North America inferred from stable isotope ratios in perissodactyl tooth enamel. Palaeogeogr. Palaeoclimatol. Palaeoecol. 417, 561–568. https://doi.org/10.1016/j.palaeo.2014.10.024.

Zanazzi, A., Fletcher, A., Peretto, C., Thun Hohenstein, U., 2022. Middle Pleistocene paleoclimate and paleoenvironment of central Italy and their relationship with hominin migrations and evolution. Quat. Int. 619, 12–29. https://doi.org/10.1016/j.quaint.2022.01.011.

Zazzo, A., Balasse, M., Patterson, W.P., 2005. High-resolution $\delta^{13}C$ intratooth profiles in bovine enamel: Implications for mineralization pattern and isotopic attenuation. Geochem. Cosmochim. Acta 69, 3631–3642. https://doi.org/10.1016/j.gca.2005.02.031.

Zhang, C., Wang, Y., Li, Q., Wang, X., Deng, T., Tseng, Z.J., Takeuchi, G.T., Xie, G., Xu, Y., 2012. Diets and environments of late Cenozoic mammals in the Qaidam Basin, Tibetan Plateau: Evidence from stable isotopes. Earth Planet Sci. Lett. 333–334, 70–82. https://doi.org/10.1016/j.epsl.2012.04.013.

Zin-Maung-Maung-Thein, Takai, M., Uno, H., Wynn, J.G., Egi, N., Tsubamoto, T., Thaung-Htike, Aung-Naing-Soe, Maung-Maung, Nishimura, T., Yoneda, M., 2011. Stable isotope analysis of the tooth enamel of Chaingzauk mammalian fauna (late Neogene, Myanmar) and its implication to paleoenvironment and paleogeography. Palaeogeogr. Palaeoclimatol. Palaeoecol. 300, 11–22. https://doi.org/10.1016/j.palaeo.2010.11.016.